

Manuscript Details

Manuscript number	ENVPOL_2018_2272_R2
Title	Plastic-associated harmful microalgal assemblages in marine environment
Article type	Research Paper

Abstract

Plastic debris carry fouling a variety of class-size organisms, among them harmful microorganisms that potentially play a role in the dispersal of allochthonous species and toxic compounds with ecological impacts on the marine environment and human health. We analyzed samples of marine plastics floating at the sea surface using a molecular qPCR assay to quantify the attached microalgal taxa, in particular, harmful species. Diatoms were the most abundant group of plastic colonizers with maximum abundance of 8.2×10^4 cells cm^{-2} of plastics, the maximum abundance of dinoflagellates amounted to 1.1×10^3 cells cm^{-2} of plastics. The most abundant harmful microalgal taxon was the diatom *Pseudo-nitzschia* spp., including at least 12 toxic species, and the dinoflagellate *Ostreopsis* cf. *ovata* with 6606 and 259 cells cm^{-2} , respectively. The abundance of other harmful microalgal species including the toxic allochthonous dinoflagellate *Alexandrium pacificum* ranged from 1 to 73 cells cm^{-2} . In the present study, a direct relationship between the abundance of harmful algal species colonizing the plastic substrates and their toxin production was found. The levels of potential toxins on plastic samples ranged from 101 to 102 ng cm^{-2} , considering the various toxin families produced by the colonized harmful microalgal species. We also measured the rate of adhesion by several target microalgal species. It ranged from 1.8 to 0.3 day⁻¹ demonstrating the capacity of plastic substrate colonizing rapidly by microalgae. The present study reports the first estimates of molecular quantification of microorganisms including toxin producing species that can colonize plastics. Such findings provide important insights for improving the monitoring practice of plastics and illustrate how the epi-plastic community can exacerbate the harmful effects of plastics by dispersal, acting as an alien and toxic species carrier and potentially being ingested through the marine trophic web.

Keywords assemblages; dispersal; harmful algae; biotoxins; marine plastics; qPCR

Corresponding Author Antonella Penna

Corresponding Author's Institution University of Urbino

Order of Authors Silvia Casabianca, Samuela Capellacci, Maria Grazia Giacobbe, Carmela Dell'Aversano, Fabio Varriale, Luciana Tartaglione, Riccardo Narizzano, Fulvia Risso, Paolo Moretto, Alessandro Dagnino, Rosella Bertolotto, Enrico Barbone, Nicola Ungaro, Antonella Penna

Suggested reviewers shauna murray, Andy Turner, Ilaria Corsi, Salvatrice Vizzini, Per Juel Hansen, luigi vezzulli

Submission Files Included in this PDF

File Name [File Type]

Cover Letter.docx [Cover Letter]

Reviewers replies II.docx [Response to Reviewers]

HIGH-LIGHTS.docx [Highlights]

graphical abstract.pdf [Graphical Abstract]

ms_19092018.docx [Manuscript File]

Supplementary Material.docx [Supporting File]

To view all the submission files, including those not included in the PDF, click on the manuscript title on your EVISE Homepage, then click 'Download zip file'.

Research Data Related to this Submission

There are no linked research data sets for this submission. The following reason is given:
Data will be made available on request

HIGHLIGHTS

- Toxic microalgal species colonized on marine plastic debris.
- Colonized toxic microalgal taxa on marine plastics was quantified by qPCR.
- *Pseudo-nitzschia* spp. were the predominant microalgal taxon on marine plastics.
- Concentrations of toxins on marine plastics ranged from 10^1 to 10^2 ng cm⁻².
- Harmful Algal species can be dispersed through plastics in marine environment.

1 **Plastic-associated harmful microalgal assemblages in marine environment**

2

3 Silvia Casabianca^{‡#}, Samuela Capellacci^{‡#}, Maria Grazia Giacobbe^f, Carmela Dell'Aversano^{‡#},
4 Luciana Tartaglione^{‡#}, Fabio Varriale[‡], Riccardo Narizzano[‡], Fulvia Risso[‡], Paolo Moretto[‡],
5 Alessandro Dagnino[‡], Rosella Bertolotto[‡], Enrico Barbone[∞], Nicola Ungaro[∞], Antonella Penna^{‡,#,γ*}

6

7 [‡]Department of Biomolecular Sciences, University of Urbino, 61121 Pesaro, Italy

8 ^fISMAR CNR, Istituto per l'Ambiente Costiero, Consiglio Nazionale delle Ricerche, Messina, Italy

9 [‡]Department of Pharmacy, University of Napoli Federico II, 80131 Napoli, Italy.

10 [‡]Agenzia Regionale per la Protezione dell'Ambiente Ligure (ARPAL), Genova, Italy

11 [∞]Agenzia Regionale per la Protezione dell'Ambiente Puglia (ARPA Puglia), Bari, Italy

12 [#]CONISMA, Consorzio Interuniversitario Scienze del Mare, 00184 Roma, Italy

13 ^γISMAR CNR, Istituto di Scienze Marine, Consiglio Nazionale delle Ricerche, Ancona, Italy

14

15 *corresponding author: Antonella Penna, University of Urbino, Viale Trieste 296, 61121 Pesaro
16 (PU), Italy, Phone 00390722304908; email: antonella.penna@uniurb.it

17

18 **Declaration of interest:** none.

19

20

21 Abstract

22 Plastic debris carry fouling a variety of class-size organisms, among them harmful microorganisms
23 that potentially play a role in the dispersal of allochthonous species and toxic compounds with
24 ecological impacts on the marine environment and human health. We analyzed samples of marine
25 plastics floating at the sea surface using a molecular qPCR assay to quantify the attached microalgal
26 taxa, in particular, harmful species. Diatoms were the most abundant group of plastic colonizers
27 with maximum abundance of 8.2×10^4 cells cm^{-2} of plastics, the maximum abundance of
28 dinoflagellates amounted to 1.1×10^3 cells cm^{-2} of plastics. The most abundant harmful microalgal
29 taxon was the diatom *Pseudo-nitzschia* spp., including at least 12 toxic species, and the
30 dinoflagellate *Ostreopsis* cf. *ovata* with 6606 and 259 cells cm^{-2} , respectively. The abundance of
31 other harmful microalgal species including the toxic allochthonous dinoflagellate *Alexandrium*
32 *pacificum* ranged from 1 to 73 cells cm^{-2} . In the present study, a direct relationship between the
33 abundance of harmful algal species colonizing the plastic substrates and their toxin production was
34 found. The levels of potential toxins on plastic samples ranged from 10^1 to 10^2 ng cm^{-2} , considering
35 the various toxin families produced by the colonized harmful microalgal species. We also measured
36 the rate of adhesion by several target microalgal species. It ranged from 1.8 to 0.3 day^{-1}
37 demonstrating the capacity of plastic substrate colonizing rapidly by microalgae. The present study
38 reports the first estimates of molecular quantification of microorganisms including toxin producing
39 species that can colonize plastics. Such findings provide important insights for improving the
40 monitoring practice of plastics and illustrate how the epi-plastic community can exacerbate the
41 harmful effects of plastics by dispersal, acting as an alien and toxic species carrier and potentially
42 being ingested through the marine trophic web.

43

44 **Plastics contribute to disperse species-specific toxic and allochthonous microalgae and**
45 **biotoxins in the marine environment**

46

47 *Keywords:* assemblages, dispersal, harmful algae, biotoxins, marine plastics, qPCR

48

49

50

51 **1. Introduction**

52 It has been estimated that 23,150 of the 268,940 tons of plastic particles floating on the surface of
53 the world's oceans are found on the Mediterranean Sea surface (Lebreton et al., 2012; Eriksen et al,
54 2014). This global issue is coming to the fore, with mounting evidence of how plastic pollution
55 affects the marine ecosystem and the food web. The growing production of plastics is undoubtedly
56 related to the expanding human consumption (Derraik, 2002; Brown et al. 2015; Jambeck et al.,
57 2015).

58 Plastics accumulate along the coasts and in open oceans through currents and gyres (Law et al.,
59 2010; Andrady, 2011) and their distribution is influenced by wind mixing, affecting their vertical
60 movement (Kukulka et al., 2012). The densities of microplastics also affect their distribution as
61 floating plastics remain on the surface, whereas their denser counterparts fall to the sea floor
62 (Engler, 2012). Further, it is known that plastic debris can persist at the sea surface for years or even
63 decades due to the stability of plastics and nature of the material that was composed by polymers
64 having less density than seawater (Andrady et al., 2011; Cózar et al., 2014).

65 Floating plastics are a durable and persistent substratum for the bio-adhesion of micro- and macro-
66 organisms enabling the dispersal from native to new habitats (Reisser et al., 2014; Fazey et al.,
67 2016). Consequently, the settlement of non-indigenous organisms can potentially lead to the
68 establishment of alien communities, which may alter existing communities, introduce disease
69 vectors and facilitate the dispersal of organic pollutants accumulated from surrounding waters
70 (Zettler et al., 2013; Goldstein et al., 2014). This has already been shown to occur for bacteria,
71 plants, harmful microalgae of dinoflagellates and animals (Masó et al., 2003; De Tender et al.,
72 2015; Oberbeckmann et al., 2015).

73 In particular, microbial adhesion and colonization on plastic particles in marine environment occur
74 quickly (Bakker et al., 2003; Zettler et al., 2013; Oberbeckmann et al., 2015). Indeed, microbial
75 biofilm formation on bags can occur after a week (Lobelle and Cunliffe, 2011). The surface –
76 attached bacterial communities are able to colonize on various types of plastic materials, such as
77 PET (polyethylene terephthalate), PVC (polyvinyl chloride) and PS (polystyrene), being subjected
78 to seasonal conditions and habitat variation (Webb et al., 2009). It has also been shown that
79 biofilms on the floating plastics contain mostly diatoms, “cyanobacteria” and “coccolithophores”
80 (Briand et al., 2012; Oberbeckmann et al., 2014; Reisser et al., 2014). The biological adhesion of
81 plastic debris is mediated by their hydrophobic surface, and the microbial biofilms on microplastics
82 can affect the physical properties of plastic particles (e.g. size, weight, buoyancy) by accelerating
83 their sedimentation on the sea bottom (Salta et al., 2013; Zettler et al., 2013). The plastics may be a
84 vector for dispersal by colonized harmful microorganisms. In fact, in addition to high abundance of
85 *Vibrio* spp., *Campylobacter* spp., *Pseudomonas* spp., which have been detected, the harmful
86 dinoflagellates *Alexandrium*, *Coolia* and *Ostreopsis* have been retrieved on plastics floating in
87 coastal waters of the Mediterranean Sea (Masò et al., 2003; Zettler et al., 2013; Masò et al., 2016).
88 The relationship between an *A. taylorii* bloom event and the detection of *A. taylorii* cells attached to
89 plastic fragments has been suggested (Masó et al., 2003). Analyses of pelagic and benthic marine
90 plastic debris by scanning electron microscopy (SEM), has confirmed the presence of diatoms (100
91 - 94% of the pelagic and benthic plastics sampled, respectively), dinoflagellates (58% and 13% of
92 the pelagic and benthic plastics sampled, respectively) (Masò et al., 2016).

93 In the Mediterranean Sea, the HAB events are mostly caused by dinoflagellate species. Their
94 blooms appear to be influenced and determined by the hydrodynamic regimes of coastal areas and
95 life-history of strategies, and plastics can be subjected to the same physical processes favouring
96 their accumulation and providing substrates for microalgae proliferation (Basterretxea et al., 2007).
97 Moreover, the increasing anthropic pressures and global climate change are intensifying the HAB
98 phenomenon facilitating noxious and allochthonous species dispersal in the seas through ballast

99 waters, shellfish translocation or plastic vectors (Hamer et al., 2001; Hallegraeff, 2010; Masó et al.,
100 2016).

101 Therefore, macroplastics and microplastics pose risk to zooplankton, marine mammals, birds and
102 fishes, as well as a potential vector for the dispersal of allochthonous and harmful microorganisms
103 (Andrady, 2011; Masó et al., 2016). In particular, the harmful algal (HA) species produce a variety
104 of marine biotoxins that are always implicated in episodes of filter or grazer-feeding animal
105 contamination and human poisoning sometimes being lethal worldwide (Anderson et al., 2012;
106 Parsons et al., 2012; Trainer et al., 2012). If ingested, plastics may act as a vehicle for toxins to
107 enter the food chain. Indeed, in the micrometer range, plastics have been found to be ingested and
108 egested by the marine biota, whereas nonoplastics can pass through cell membranes, potentially
109 causing harm to organisms (Cole et al., 2013).

110 This study aims to characterize and quantify target harmful microalgal taxa, diatoms (class
111 Bacillariophyceae), and dinoflagellates (class Dinophyceae) potentially attached to micro and
112 macro plastics collected in the coastal waters and off-shore of the Mediterranean Sea using
113 molecular qPCR based assay. The investigated harmful algal taxon was the diatom *Pseudo-*
114 *nitzschia*. Genus *Pseudo-nitzschia* include at least 12 toxic species (e.g. *P. multiseriata*, *P. australis*,
115 *P. seriata* and *P. multistriata*). These species produce domoic acid (DA), a neurotoxin that cause
116 amnesic shellfish poisoning (ASP) (Trainer et al., 2012). The other studied species were the toxic
117 dinoflagellates *Alexandrium pacificum*, *A. minutum* and *Ostreopsis cf. ovata*. Both *Alexandrium*
118 species produce the PSTs (paralytic shellfish toxins), which are neurotoxins causing paralytic
119 shellfish poisoning (PSP) (Franco et al., 1994; Krock et al., 2007; Penna et al., 2015). The toxic
120 epiphytic *O. cf. ovata* produces ovatoxins (OVTXs) and palytoxin (PLTX), one of the most potent
121 non-protein marine toxins so far known (Ciminiello et al., 2012; Tartaglione et al., 2017). All these
122 harmful microalgal taxa are abundantly distributed along the coastal waters of the Mediterranean
123 Sea.

124 In the present study, all plastic samples were characterized by Fourier-transform infrared
125 spectroscopy (FTIR).

126 Furthermore, since the plastics are considered potentially vehicles for the transport of toxic
127 microorganisms, toxin levels of harmful algae collected from plastic surfaces during a HAB (harmful
128 algal bloom) event were measured by liquid chromatography coupled with high resolution mass
129 spectrometry (LC-HRMS) to determine if marine plastic debris could directly constitute a toxin
130 vector and the potential risk of the dispersion of such vectors in the marine environment.

131 In addition to these investigations in the field, *in vitro* experiments using plastic sheets and target
132 cultured harmful microalgal species were carried out to estimate the capacity and rate of adhesion
133 of toxic algal species to plastic surfaces.

134

135 **2. Materials and methods**

136 *2.1 Microalgal cultures*

137 The strains of harmful dinoflagellate *Alexandrium pacificum* (CNR-ACAT5D1, CNR-ACAT6A2,
138 CNR-ACAT6FA, CNR-ACAT6D4, CNR-ACAT7A2, CNR-ACAT6D5, CNR-ACAT15P) were
139 obtained from various plastic samples collected at the sea surface during a monospecific bloom at
140 Syracuse Bay, Ionian Sea (Italy) in the same survey of plastic debris in 2016-2017 as described
141 below. The microalgal cells were removed from plastics by gently scraping in 5 mL sterile
142 seawater. Single cells were isolated by micropipetting and clonal cultures were established and
143 maintained in F/2 (Guillard, 1975). These strains together with *A. pacificum* CNR-ACAT15, CNR-
144 ACATA1, CNR-ACAT02 strains, which were isolated from Syracuse harbour, were further
145 analysed for the PSTs (paralytic shellfish toxins) content by LC-HRMS.

146 Further, a total of 22 microalgal strains were used in the present study for plastic adhesion
147 experiments and molecular standard curves used in the qPCR quantification assay (Table S1).

148 All strains were maintained in different media at $23 \pm 1^\circ\text{C}$ and $16 \pm 1^\circ\text{C}$ for species belonging to
149 the class Dinophyceae and Bacillariophyceae, respectively. Light was provided by cool-white

150 fluorescent bulbs (photon flux of $100 \mu\text{E m}^{-2} \text{ s}^{-1}$) on a standard 14:10 h light-dark cycle. Culture
151 subsamples, each containing 1.0×10^5 cells were harvested by centrifugation (4000 rpm for 10 min)
152 during the exponential growth phase. Microalgal pellets were stored at $-80 \text{ }^\circ\text{C}$ for subsequent
153 molecular analyses for standard curves mixtures with the exception of *Pseudo-nitzschia*
154 *multistriata*, *A. pacificum* strains (CNR-ACAT5D1, CNR-ACAT6A2, CNR-ACAT6FA, CNR-
155 ACAT6D4, CNR-ACAT7A2, CNR-ACAT6D5, CNR-ACAT15P) and *Protoceratium reticulatum*.

156

157 *2.2 Environmental plastic sampling and processing*

158 A total of 42 plastic samples were collected in different areas of the Mediterranean Sea from March
159 2016 to May 2017 (Table S2). Sampling was done by the use of a manta net of $330 \mu\text{m}$ mesh size,
160 which is composed of (i) a steel mouth of about $0.50 \times 0.25 \text{ m}$ of opening, (ii) two buoyant wings,
161 (iii) a conic net about 3 m long, (iv) a collector at the code end. Manta net was towed for about 20
162 min at a speed of approximately 1.5 - 2 knots: this procedure allows manta net to float on the sea
163 with the lower half-mount under the surface. In addition, macroplastic samples, i.e. floating pieces
164 of plastic on the sea surface, were also collected manually. After the collection, micro- and
165 macroplastic samples were preserved immediately at -20°C . These micro and macroplastic samples
166 were analyzed by qPCR using length (cm^2) or weight (mg) for molecular abundance quantification
167 of attached microalgal taxa.

168 Laboratory processing and subsequent sorting of microplastics collected by the manta net was
169 carried out as follows: once placed on board, the net was rinsed with seawater from the outside
170 inwards to collect all the material captured by the net in the collector container. The container was
171 then detached from the net and the sample filtered using a sieve for discharging particles greater
172 than 5 mm size. Then, the sample was poured into a 1000 mL , 500 mL or 250 mL glass jars. Plastic
173 samples were rinsed with distilled water several times. They were then dried off at room
174 temperature for 48 hours, and stored in the dark at room temperature for subsequent chemical
175 analyses.

176

177 *2.3 FTIR spectroscopy*

178 A Nicolet 6700 FT-IR spectrometer (Thermo Fisher, USA) fitted with a single bounce attenuated
179 total reflectance (ATR) accessory was used to characterize the plastic samples. The ATR accessory
180 was equipped with zinc selenide (ZnSe) reflection crystal. ATR-FTIR spectra was collected by
181 coaddition of 32 scans at a resolution of 4 cm⁻¹ against a background spectrum from the clean ATR
182 crystal. ATR-FTIR measurements were conducted at room temperature (20°C). Spectra were
183 recorded in absorbance mode in the spectral region 4000–600 cm⁻¹. Plastic samples were analyzed
184 directly on the ZnSe ATR crystal. The sample spectra were submitted to automated library search
185 and finally the spectrum of the candidate polymer was overlaid and compared with the sample
186 spectrum to check the result.

187

188 *2.4 DNA extraction and qPCR analyses on environmental marine plastic samples*

189 Macroplastic samples were sized and bigger pieces of macroplastics were cut by sterile scissors for
190 subsequent analyses. Microplastics (< 5 mm in size) obtained from manta net sampling were used
191 directly. Genomic DNA was extracted from microalgal cultures and from marine macro and
192 microplastic samples with size range from 1.7 to 80 cm² and weight from 95 to 400 mg,
193 respectively. The genomic DNA was extracted using the DNeasy PowerSoil Kit (Qiagen, Hilden,
194 Germany), according to the manufacturer's instructions with DNA being eluted in a final volume of
195 100 µL elution buffer. DNA was quantified using a Qubit fluorometer with a Quant-iT dsDNA HS
196 assay Kit (Invitrogen, Carlsbad, CA) and stored at -20°C until PCR analysis.

197 Class-specific primers for the detection of Dinophyceae and Bacillariophyceae (Godhe et al., 2008)
198 were used for the amplification and quantification of SSU rDNA fragments obtained from several
199 different species of cultured algal strains and microalgal assemblages attached to the plastic field
200 samples. Positive plastic samples were analysed for the quantification of LSU or 5.8S-ITS rDNA

201 fragments of several target harmful dinoflagellate and diatom genera and species by qPCR based
202 assay (Table S3).

203 The qPCR assay was performed as described in Perini et al. (2018). The standard curves for the
204 copy number quantification of Dinophyceae and Bacillariophyceae classes were constructed using a
205 six point ten-fold dilution series of purified SSU rDNA PCR products (from 2 to 1.0×10^6 copies)
206 generated from DNA of *A. pacificum* CNR-SRA4 and *Chaetoceros* sp. CBA22 (Perini et al., 2018).
207 On the other hand, the species-specific standard curves of *L. polyedrum*, *A. minutum*, *A. pacificum*
208 and *O. cf. ovata* were obtained using plasmids (Perini et al., 2011; 2018), as well as those for the
209 quantification of the genus *Pseudo-nitzschia* (Penna et al., 2013).

210 Two different cellular standard curves, namely DinoMix and BaciMix, of ten-fold serial dilution in
211 the 1.0×10^{-2} - 1.0×10^3 and 1.0×10^0 - 1.0×10^3 cellular range were constructed to quantify
212 Dinophyceae and Bacillariophyceae classes in plastic field samples, respectively. Because class
213 primers were able to amplify many dinoflagellate and diatom species, the cellular standard curves
214 were obtained by mixing purified DNAs obtained from all 10 different monoclonal cultures of
215 Dinophyceae and Bacillariophyceae, respectively (Table S4). To evaluate the potential variability of
216 SSU rDNA copy number, diverse mixtures were made of the final volume of 10 μ L containing
217 different mixed amounts of genomic DNAs that were extracted from 1.0×10^5 cultured cells. The
218 mixtures were performed using various percentages of DNA ranging from 10% to 40%,
219 corresponding to 1.0×10^3 to 4.0×10^3 cells.

220 Acquisition of qPCR data and subsequent analyses were carried out using StepOne software ver.
221 2.3. A dissociation curve was generated after each amplification run to check for amplicon
222 specificity and primer dimers. The automatically generated standard curves were accepted when the
223 slope was between - 3.32 and - 3.55 (100 – 91% efficiency) and the correlation coefficient (R^2) was
224 at least 0.99. An estimation of the SSU rDNA copies cm^{-2} and copies mg^{-1} was provided for
225 Dinophyceae and Bacillariophyceae classes. The quantification of phytoplankton species by class
226 primers was performed using DinoMix and BaciMix cellular curves. Dinophyceae and

227 Bacillariophyceae abundance was calculated by plotting the Ct (threshold cycle) values of
228 environmental plastic samples on the cellular standard curves, taking into account the DNA elution
229 volume and dilution factors. The previously described standard curves were used for the
230 quantification of the copy number of both cultured strains and purified cells from environmental
231 plastic samples by qPCR. Taking into account the dilution factor, the total copy number in each
232 sample was obtained. This value was finally divided by the copy number per cell, derived from
233 cultured strains of the different species. The abundance of Dinophyceae, Bacillariophyceae and the
234 other harmful algal species attached to plastic samples was normalized to cells cm⁻² and cells mg⁻¹
235 for macroplastic or microplastic samples. Statistical analyses were performed with non parametric
236 Mann–Whitney, Kruskal Wallis and Spearman correlation tests using PAST ver. 3.14 with a p-
237 value < 0.05 determining significance.

238

239 *2.5 Extraction of algal pellet and Liquid Chromatography-High Resolution Multiple Stage Mass* 240 *Spectrometry (LC-HRMSⁿ, n=2)*

241 A total of 10 *A. pacificum* cultured strains (Table S1) at a cellular concentration from 1.5 x 10⁶ to
242 1.0 x 10⁷, was collected during the exponential growth phase, centrifuged at 4000 rpm for 15 min
243 and the pellets were then frozen at -80°C until chemical analyses. Water, acetonitrile and methanol
244 (HPLC grade), glacial acetic acid and formic acid (Laboratory grade) were purchased from Sigma-
245 Aldrich Corporation (St. Louis, MO). A 25% ammonia solution (LC-MS grade) was obtained from
246 Merck Millipore (Germany). Standard solutions of PST (paralytic shellfish toxin) were obtained
247 from the NRC Certified Reference Materials (CRM) Program (Halifax, NS, Canada).

248 The 10 pellets of *A. pacificum* were separately extracted with 0.5 mL of 0.1 M acetic acid in water,
249 while being sonicated for 10 min in pulse mode in an ice bath. The mixture was centrifuged at 8000
250 rpm for 10 min and the supernatant was decanted. Each residue was extracted once again with 0.5
251 mL of the extraction solvent, the supernatant was decanted and the two extracts were combined (1

252 mL total). A 50 μ L of each extract was added to 150 μ L of acetonitrile and subsequently
253 analyzed by HILIC-HRMSⁿ (5 μ L injected).

254 A Dionex Ultimate 3000 quaternary system coupled with a hybrid linear ion trap LTQ Orbitrap
255 XLTM Fourier Transform MS (FTMS) equipped with an ESI ION MAXTM source (Thermo-Fisher,
256 San Jose, CA, USA) was used. For PST HILIC – HRMSⁿ separations were performed according to
257 Turner et al. (2017) with slight modifications. A Water Acquity UPLC BEH Glycan 1.7 μ m, 2.1 x
258 150 mm column (Batch 0161) was used in conjunction with a Waters VanGuard BEH Amide
259 cartridge 1.7 μ m, 2.1 x 5 mm (Waters, Massachusetts, USA) maintained at 60°C. The column was
260 eluted with water + 0.015% formic acid + 0.06% ammonia 25% (eluent A) and 70%
261 acetonitrile/water + 0.01% formic acid (eluent B) according to the following gradient: time (t)= 0
262 min, 99% B; t= 10 min, 99% B; t= 15 min, 50% B; t= 18 min, 50% B; t=19 min, 99% B; t=20 min,
263 99% B. A flow rate of 0.20 mL/min was used for the first 15 min and of 0.25 mL/min for the rest of
264 the acquisition time. Re-equilibration time at the initial conditions was 12 min.

265 In all cases, HRMSⁿ analyses (n = 1-3) were performed in positive ion mode at a resolving power of
266 60,000 (FWHM at m/z 400) and a spray voltage of 4.8 kV. PST detection was accomplished in
267 collision induced dissociation (CID) MS² mode using the following source settings: capillary
268 temperature = 220 °C, capillary voltage = 49 V, sheath gas = 62 and auxiliary gas= 16.5 (arbitrary
269 units), tube lens voltage= 250 V; an activation Q of 0.250, and an activation time of 30 ms using
270 collision energies in the range 22–28%. The tube lens voltage was set at 120 V. Extracted ion
271 chromatograms (XIC) of the fragment ions of PST (Perini et al., 2014) were obtained at a 5 ppm
272 mass tolerance and used for quantification. Quantification of the toxins was accomplished by direct
273 comparison of XIC areas of individual toxins to relevant PST CRM solutions injected at similar
274 concentrations injected under the same experimental conditions. The results were expressed on a
275 per cell basis (fg cell⁻¹).

276

277 *2.6 Adhesion rate of harmful algal species to the plastic substrate*

278 Each strain of the diatoms *P. multistriata* CBA174, *Skeletonema marinoi* CBA4, and the
279 dinoflagellates *A. minutum* CBA57, *A. pacificum* CNR-SRA4, *L. polyedrum* LPA0510, *P.*
280 *reticulatum* PRA0311, *G. spinifera* CBA5 and *O. cf. ovata* CBA1291 were grown in 1 L glass
281 bottles containing 0.4 L of sterilized medium together with sterilized PE plastic sheets (3 cm x 3
282 cm), which were cut from bigger fragments collected previously along the shoreline. The initial cell
283 number was the same for all the selected strains (1.0×10^3 cells mL⁻¹). Culture media conditions
284 were those described above. A plastic sheet was harvested every four days from the inoculum and
285 gently scraped in 10 mL of sterile seawater 0.45 µm filtered using a spatula in order to recover the
286 cells adhering to the plastic sheets. Subsamples of 1 mL were collected for cell density estimation
287 using Sedgewick-Rafter counting chamber. Cell amount was estimated using an inverted
288 microscope (ZEISS Axiovert 40CFL) at 400X magnification. The adhesion rates, defined as the rate
289 of increased abundance on the plastic sheets, were calculated on the basis of the longest possible
290 period of exponential growth using the equation: $\mu = \ln(Nt/N0)/\Delta t$, where N is the number of the
291 plastic adherent cells expressed as cells cm⁻² and Δt is the time interval expressed in days (Wood et
292 al., 2005).

293

294

295 **3. Results**

296 *3.1 Plastic type and structure analysis*

297 The amount of sampled microplastics corresponding to a 64% was non-polar (polyethylene and
298 polypropylene) with a typical crystalline structure, the remaining 36% had a certain level of polarity
299 with a typical amorphous structure (Fig. 1). Detailed ATR-FTIR spectra of analysed plastic samples
300 were shown in Figs. S1-S6.

301

302 *3.2 Molecular quantification of microalgal assemblages and harmful algal taxa on marine plastics*

303 *3.2.1 Dinophyceae and Bacillariophyceae standard curve characterization*

304 The mean standard curves of Dinophyceae and Bacillariophyceae showed a PCR efficiency of 93
305 and 99% respectively ($y = -3.49x + 35.21$; $y = -3.36x + 38.86$ for Dinophyceae and
306 Bacillariophyceae, respectively), a linear correlation of 6 \log_{10} ($R^2 = 0.99$) and a sensitivity of 2
307 copies/reaction (Ct mean = 33.03 ± 0.88 and Ct mean = 36.76 ± 0.34 for Dinophyceae and
308 Bacillariophyceae, respectively). The reproducibility was also assayed and the CV_{Ct} mean values
309 were 1% and 11% ($1.0 \times 10^6 - 2.0 \times 10^0$ molecules), for Dinophyceae and Bacillariophyceae
310 respectively, while, the CV_{Cn} mean values were 18% and 9%, for Dinophyceae and
311 Bacillariophyceae, respectively. Species-specific standard curve characterization of *A. pacificum*, *A.*
312 *minutum*, *L. polyedrum*, *P. reticulatum* and *G. spinifera* are reported in Perini et al. (2018), while
313 the standard curve of *Pseudo-nitzschia* spp. and *O. cf. ovata* are described in Penna et al. (2013) and
314 Perini et al. (2011), respectively.

315

316 3.2.2 The qPCR assay of DNA mixtures of Dinophyceae and Bacillariophyceae

317 The different mixtures assembled using variable percentage of DNA from a known number of
318 cultured cells of various species of Dinophyceae and Bacillariophyceae were analyzed by qPCR
319 assay, and the obtained Ct values showed no significant differences ($H_c = 2.554$, $p = 0.278$ and H_c
320 $= 2.333$, $p = 0.312$ for Dinophyceae and Bacillariophyceae, respectively) allowing the use of these
321 mixtures for the construction of DinoMix and BaciMix standard curves.

322 The cellular standard curves used for the quantification of Dinophyceae and Bacillariophyceae
323 classes showed a PCR efficiency of 100 – 91% ($y = -3.322x + 28.60$ and $y = -3.549x + 33.84$,
324 respectively), a linear correlation of 5 or 4 \log_{10} ($R^2 = 0.99$) and a quantification limit of 0.01 (Ct
325 mean = 34.49 ± 0.48) and one cell (Ct mean = 33.66 ± 0.22) per PCR reaction for Dinophyceae and
326 Bacillariophyceae, respectively. The reproducibility, analyzed as CV_{Ct} mean inter-assay variability
327 of different cellular standard curves was 0.6% (range 0.01 - 1000 cells) for Dinophyceae and 0.4%
328 (range 1 - 1000 cells) for Bacillariophyceae.

329

330 3.2.3 The qPCR assay for harmful microalgal species quantification on plastics

331 All the 42 plastic samples tested positive for the presence of Dinophyceae and Bacillariophyceae
332 (Fig. 2). The total SSU rDNA copy number and abundance of both dinoflagellates and diatoms
333 attached to the plastics determined by qPCR assay were plotted. The major axis regression between
334 cell concentration and rDNA copy number assessed by qPCR showed a highly significant linear
335 correlation: $n = 33$, Spearman $r_s = 0.9983$, $p \ll 0.001$ for dinoflagellate abundance determined per
336 cm^{-2} ; $n = 9$, Spearman $r_s = 0.9832$, $p \ll 0.001$ for dinoflagellate abundance determined per mg^{-1} ; n
337 $= 33$ Spearman $r_s = 0.9996$, $p \ll 0.001$ for diatom abundance per cm^{-2} ; $n = 9$, Spearman $r_s =$
338 0.9748 , $p < 0.001$ for diatom abundance determined per mg^{-1} .

339 All the plastic samples were quantified for the presence of Dinophyceae. They showed variable
340 amount values that were expressed both as cellular abundance or copy number. These values ranged
341 from 1 to 1.1×10^3 cells cm^{-2} and 1 to 61 cells mg^{-1} or from 38 to 8.3×10^4 SSU rDNA copy
342 number cm^{-2} and 8 to 4.0×10^3 LSU rDNA copy number mg^{-1} . Six samples showed very low
343 Dinophyceae abundance, as one cell cm^{-2} or 73 ± 30 copy number cm^{-2} (samples 9, 16, 23) and
344 one cell mg^{-1} or 14 ± 6 copy number mg^{-1} (samples 1, 2, 15). Indeed, the Bacillariophyceae showed
345 a higher number of cells attached to the plastics than did Dinophyceae with values ranging from 1
346 to 8.2×10^4 cells cm^{-2} and 1 to 2.1×10^2 cells mg^{-1} or of 43 to 3.6×10^6 SSU rDNA copy number
347 cm^{-2} and 10 to 8.6×10^3 SSU rDNA copy number mg^{-1} . Using this molecular assay, the
348 quantification of a single cell was feasible. One cell cm^{-2} (43 ± 8 copy number cm^{-2}) and one
349 cell/mg (20 ± 14 copy number mg^{-1}) was found in the analysed environmental samples (36 and 2,
350 and 29, respectively). Furthermore, all plastic samples were analyzed for the quantification of
351 harmful target microalgal taxa, namely *A. pacificum*, *A. minutum*, *O. cf. ovata*, and *Pseudo-*
352 *nitzschia* spp. (Fig. 3). Sixteen plastic samples showed the presence of the toxic and allochthonous
353 *A. pacificum* and higher amounts were found in sample 33 from Syracuse (Ionian Sea) with 30 cells
354 cm^{-2} . Samples 17, 19 and 21 contained an abundance of *A. pacificum* in the range of 3 - 28 cells cm
355 $^{-2}$, while the remaining samples showed amount of one cell cm^{-2} . Sample 32 showed one cell mg^{-1}

356 of *A. pacificum*. Nine samples tested positive for the presence of *A. minutum* with the highest
357 abundance found in sample 33 from the Syracuse site showing 73 cells cm⁻². Samples 31 and 37
358 contained 7 and 13 cells cm⁻² of *A. minutum*, respectively. Sample 32 showed one cell mg⁻¹ of *A.*
359 *minutum*. The highest abundance of *O. cf. ovata* was found in sample 22 from the Taormina site
360 (Ionian Sea) with 259 cells cm⁻², the remaining samples from the same site showed a cell range of
361 1 - 9 cells cm⁻². Sample 29 showed one cell/mg of *O. cf. ovata*. *Pseudo-nitzschia* spp. was present
362 in almost all plastic samples resulted positive for Bacillariophyceae (n = 31) with cellular values
363 ranging from 1 to 6.6 x 10³ cells cm⁻². Three samples showed one cell cm⁻² (samples 16, 23, 36).
364 Sample 32 showed one cell mg⁻¹ of *Pseudo-nitzschia* spp. Moreover, *L. polyedrum*, *P. reticulatum*
365 and *G. spinifera* were also investigated and showed scarce or low abundance. One cell cm⁻² of *L.*
366 *polyedrum* was found in samples from the Syracuse site (samples 31 - 39), with the exception of
367 sample 32, which showed one cell mg⁻¹. One cell cm⁻² of *G. spinifera* was found at the Taormina
368 (sample 25) and Bari sites (sample 16), and one cell mg⁻¹ was found at Genoa site (sample 4). No
369 amplification was obtained for *P. reticulatum* (data not shown).

370

371 3.3 Toxin content of cultured *A. pacificum* strains isolated from plastic debris

372 All the 10 strains of *A. pacificum* produced PST (Table 1), with a total toxin content in the range
373 35.14-6032 fg cell⁻¹; CNR-ACAT6FA was the most productive strain, while CNR-ACAT5D1 was
374 the least productive one. A rather high variability in toxin profiles and the relative abundance of
375 individual analogues was observed. Most of the strains produced GTX5, C1/2, GTX1/4, and
376 GTX2/3. STX was produced by 5 out of 10 strains, while dcGTX2 and NEO were found in just one
377 strain; dcGTX3 and dcNEO were absent in all the strains. As for the relative abundance of
378 individual toxins, C2 accounted for 10-56% of the total toxin content, GTX1 for 14-79%, and
379 GTX5 for 1-56%.

380

381 3.4 Adhesion rate of harmful algal species on plastic surface

382 The Kruskal Wallis test showed that the adhesion rates of target harmful algal target species varied
383 significantly ($H_c = 17.73$ $p < 0.05$). Moreover, the *a posteriori* pairwise Mann-Whitney test showed
384 that the differences between the algal species were significant ($p < 0.05$) with the exception of two
385 species as *A. minutum* and *O. cf. ovata*. The dinoflagellate *A. pacificum* appeared to be the species
386 that adhered to the plastics the most rapidly, followed by the diatoms *S. marinoi* and *P. multistriata*.
387 The species that adhered at the slowest rate were *A. minutum* and *O. cf. ovata* (Fig. 4). The other
388 investigated harmful species, namely *L. polyedrum*, *G. spinifera* and *P. reticulatum* showed
389 adhesion rates much lower than 0.1 day^{-1} (data not shown). Moreover, the maximum abundance of
390 attached cells to the plastics determined by microscopy were $3.1 \times 10^5 \pm 1.5 \times 10^4$, $2.8 \times 10^4 \pm 1.6 \times$
391 10^3 , $6.0 \times 10^3 \pm 3.4 \times 10^2$, $2.5 \times 10^3 \pm 1.5 \times 10^2$, $5.6 \times 10^2 \pm 3.3 \times 10^1$ cells cm^{-2} for *P. multistriata*, *S.*
392 *marinoi*, *A. pacificum*, *O. cf. ovata* and *A. minutum*, respectively.

393

394 4. Discussion

395 In the present study, the molecular quantification by qPCR analysis of the microalgal assemblages
396 on micro and macroplastic debris across different areas within the Mediterranean Sea provided for
397 the first time the evidence that also toxic microalgal species can colonize plastics in high amount
398 and can be dispersed through an alternative substrate. The dispersal of these associated HAB
399 microorganisms across the ocean by currents and winds can be facilitated by floating plastics,
400 because they are persistent, widespread and have various shape and size (Kiessling et al., 2015).

401 In the present study, we showed that the communities of Bacillariophyceae and Dinophyceae were
402 attached to all the plastic samples that were analyzed using the molecular qPCR assay. The
403 abundance of the communities was highly variable with Bacillariophyceae showing up to 10^4 cells
404 cm^{-2} or 10^2 cells mg^{-1} and Dinophyceae showing 10^3 cells cm^{-2} or 61 cells mg^{-1} . The numerical
405 variability and the observed composition of microalgal assemblages were probably related to the
406 dispersion rate and period of time the plastics were floating in the areas where the plastics were
407 collected. In the present study, Bacillariophyceae showed the highest abundance of cells attached to

408 plastics in the areas in the Mediterranean Sea where samples were collected. This is consistent with
409 recent findings regarding the diatom microbiota found attached to plastic debris and analysed using
410 other techniques, such as SEM or metabarcoding qualitative analysis (Farrell et al., 2013; Zettler et
411 al., 2013). Diatoms are probably more able to form biofilms on plastics by producing extracellular
412 substances, which can further facilitate their colonization and the colonization or grazing of other
413 organisms (Reisser et al., 2014). Thus, diatom fouling seems to retain high diversity and to be
414 widespread on marine plastics. However, it is not yet known if the relationship between grazers and
415 plastics has a positive or negative impact on the new marine food web considering that plastics can
416 retain toxic compounds (Cole et al., 2013). Within the Bacillariophyceae, the potentially toxic
417 complex of the *Pseudo-nitzschia* spp. showed the highest abundance of cells attached to the plastic
418 sheets. Indeed, also from the *in vitro* experiments of plastic adhesion rate, the algal species that
419 showed the highest rate of adhesion were the diatoms *S. marinoi*, which is known to form high
420 density blooms and producing noxious effect on copepods by the production of polyunsaturated
421 aldehydes (Ianora et al., 2004; Lauritano et al., 2016), and the potentially toxic *P. multistriata* (data
422 not shown) with the highest maximum abundance of 10^4 and 10^5 cells cm^{-2} , respectively.

423 On the other hand, Dinophyceae showed lower abundance than Bacillariophyceae on field marine
424 plastics, but the harmful dinoflagellate investigated species such as *A. pacificum*, *A. minutum* and *O.*
425 *cf. ovata* were able to attach to the environmental plastics. In the present study, the *in vitro*
426 experiments showed that the potentially allochthonous and PSP producing dinoflagellate species *A.*
427 *pacificum* attached (with maximum abundance of 6.0×10^3 cells cm^{-2}) to the surface of the plastic
428 sheets more quickly than other microalgal species. The potentially allochthonous and toxic *A.*
429 *pacificum* blooms regularly in semi closed coastal areas of the Mediterranean Sea (Penna et al.,
430 2005; 2015) characterized by high surface temperature and the trophic input of nutrients (Bravo et
431 al., 2010). Its blooms are always correlated with the potential of PSP toxin contamination of
432 shellfish (Farrell et al., 2013). The recent dispersal of *A. pacificum* from the western Mediterranean
433 to the central areas (Penna et al., 2015) may have occurred naturally or through anthropically

434 mediated factors, such as ballast waters, aquaculture activities and plastic pollution (Masó et al.,
435 2016). Indeed, the other toxic dinoflagellate *O. cf. ovata* and *A. minutum*, which are responsible for
436 large toxic blooms along the Mediterranean coasts (Vila et al., 2005; Tartaglione et al., 2017),
437 appeared to have a lower rate of adhesion to the plastics, but still showed a valid adhesion potential
438 of 10^3 and 10^2 cells cm^{-2} maximum abundance, respectively. *Ostreopsis cf. ovata* is already known
439 to grow on different substrates, such as macrophytes and hard substrates (e.g., rocks, sand and
440 mollusc shells) (Totti et al., 2010) and the biofilm formation observed in our experiments confirmed
441 its ability to grow also on plastic sheet substrates and hence its potential dispersal through benthic
442 and floating plastic sheets. Furthermore, *Alexandrium* species and dinoflagellate resting cysts have
443 already been found on floating plastic marine debris and accumulating along shorelines of the
444 Mediterranean Sea (Masó et al., 2003). Therefore, it is likely that *A. minutum* also has the ability to
445 adhere to plastics. Furthermore, it has already been shown that the phyto - benthic and -plankton
446 communities can attach to both micro and macro plastics (Masó et al., 2016). The specific
447 properties of marine plastics seem to influence colonization and succession processes, and thus the
448 composition of associated rafting community (Kiessling et al., 2015). This could explain the
449 species-specific adhesion of harmful microalgal species shown in the present study. In fact, the
450 qPCR assay was also applied for the specific quantification of other harmful microalgal taxa on
451 surface marine plastics; these species, on the contrary, were quantified in few amounts or were not
452 detectable, such as *L. polyedrum*, *G. spinifera* or *P. reticulatum*, respectively.

453 Thus, using a qPCR approach we were able to show that some target HA species adhere tightly to
454 floating plastic debris, which suggests that the selected harmful microalgal species could potentially
455 spread through marine ecosystems and the trophic chain negatively impacting human health and
456 environment.

457 In fact, if we consider the total toxin concentration ranges of any of the toxic compounds produced
458 by the various harmful species, significant amounts of biotoxin can be dispersed in the ocean by the
459 microorganism producers attached to the plastics. In the present study, we found that the genus

460 *Pseudo-nitzschia*, which includes toxic species (i.e. *P. multiseriata*, *P. australis*, *P. seriata* and *P.*
461 *multistriata*) were the taxon attached to the plastics showing the highest cellular values, and we
462 hypothesized that *Pseudo-nitzschia* can potentially contribute to domoic acid transport with values
463 in the range of 5 - 443 ng cm⁻² on floating plastics based on the literature values (Trainer et al.,
464 2012). Indeed, based on the maximum abundance of 259 cells cm⁻² of *O. cf. ovata* found on the
465 plastics, we can hypothesize that at least 1 - 62 ng PLTX compounds cm⁻² must be accumulated in
466 floating plastics debris as established by the recent data of the Mediterranean PLTX production by
467 *O. cf. ovata* (Accoroni et al., 2011; Ciminiello et al. 2012; Brissard et al., 2014; Tartaglione et al.,
468 2017). From this study, we can assume that the PSP producing species such as *A. minutum* and *A.*
469 *pacificum*, could transport 1 – 72 pg cm⁻² of PST, respectively (see also Touzet et al., 2007;
470 Anderson et al., 2012; Pistocchi et al., 2012).

471 It is known that chemical hazards are associated with plastic debris in the marine environment
472 (Rochman, 2015). Marine plastic debris can be linked to a mixture of chemicals that can include
473 marine biotoxins. These chemical compounds produced by microalgae attached to the plastic
474 surface can be transferred throughout lower trophic level organisms as zooplankton by grazing to
475 higher trophic level organisms, which represent contaminated seafood for humans. Also filter
476 feeding animals (i.e. shellfish) can accumulate microplastics that can be colonized by toxic
477 microalgae and thus, they can represent potentially contaminating seafood to humans (Kießling et
478 al., 2015).

479 Here, there may be a potential risk of indirect toxin accumulation on plastics in the investigated
480 areas of Mediterranean Sea. Obviously, this is a prudent estimate because it does not take into
481 account the length of time that plastics are in the water. But, it is already known that plastic
482 substrata can persist in seawater for years or decades. The plastic properties of buoyancy and
483 resistance of decay make these abiotic substrata more resistant than other biotic substrata (wood,
484 macroalgae) allowing the adhesion of microorganism communities, including allochthonous
485 species, and transport for long distance of organisms that can survive for prolonged time (Pegram

486 and Andrady, 1989; Thiel and Gutow, 2005). Therefore, marine plastics may act as both sink and
487 source for chemical contaminants including their transfer into marine foodwebs (Rochman, 2015).
488 Hence, it needs urgently to acquire information on the environmental fate of biotoxins associated to
489 plastic debris in the sea.

490 In the present study, this qPCR based assay of plastics has the advantage of being able to quantify
491 the main phytoplankton groups and harmful taxa on any plastic surface debris floating on the
492 surface of the seawater. The qPCR assay can support biological monitoring of plastic debris using
493 taxon specific primers or probes for microorganisms attached to the plastics achieving high
494 detection sensitivity and specificity (up to one cell cm⁻² or mg⁻¹).

495

496 **5. Conclusions**

497 New information was obtained regarding the quantities of noxious microbiota attached to the
498 plastics floating in the Mediterranean Sea based on taxa specific rDNA gene. These findings
499 illustrate the potential risk of truly harmful microorganism dispersal associated with plastic
500 pollution. HA dinoflagellate species abundance was found to be lower than that of diatom
501 communities; however, these diatom communities include potentially toxic *Pseudo-nitzschia* spp.
502 Moreover, in high biomass blooming events, when plastic debris remains longer in the water
503 column, the potential risk of the transport of large amounts of toxins is likely.

504 In short, in view of recent findings pointing to the association of toxic biofilms with marine plastics,
505 their ingestion through the trophic web and the consequent implications for human health, measures
506 for preventing and managing plastic pollution are urgently needed.

507

508

509 **ACKNOWLEDGMENTS**

510 This work was supported by Regione Marche Project Coastal Monitoring n. 49 of 23/12/2013 of
511 Tabella C and EU ENPI CBC-MED M3-HABs Project.

512 **References**

513

514 Accoroni S., Romagnoli T., Colombo F., Pennesi C., Di Camillo C.G., Marini M., Battocchi C.,
515 Ciminiello P., Dell'Aversano C., Dello Iacovo E., Fattorusso E., Tartaglione L., Penna A., Totti
516 C., 2011. *Ostreopsis* cf. *ovata* bloom in the northern Adriatic Sea during summer 2009:
517 Ecology, molecular characterization and toxin profile. *Marine Pollution Bulletin* 62(11), 2512-
518 2519.

519

520 Anderson, D.M., Alpermann, T.J., Cembella, A.D., Collos, Y., Masseret, E., Montresor, M., 2012.
521 The globally distributed genus *Alexandrium*: Multifaceted roles in marine ecosystems and
522 impacts on human health. *Harmful Algae* 14, 10–35. <https://doi.org/10.1016/j.hal.2011.10.012>.

523

524 Andrady, A.L., 2011. Microplastics in the marine environment. *Mar. Pollut. Bull.* 62, 1596-1605.
525 <http://dx.doi.org/10.1016/j.marpolbul.2011.05.030>.

526

527 Bakker, D. P., Klijnsstra, J. W., Busscher, H. J., van der Mei, H. C. 2003. The effect of dissolved
528 organic carbon on bacterial adhesion to conditioning films adsorbed on glass from natural
529 seawater collected during different seasons. *Biofouling* 19, 391. doi:10.1080/
530 08927010310001634898

531

532 Basterretxea, G., Garcés, E., Jordi, A., Anglés, S., Masò, M., 2007. Modulation of nearshore
533 harmful algal blooms by in situ growth rate and water renewal. *Mar. Ecol. Progr. Ser.* 62, 1-12.
534 <http://dx.doi.org/10.1016/j.ecss.2004.07.008>.

535

536 Bravo, I., Fraga, S., Figueroa, R.I., Pazos, Y., Massanet, A., Ramilo, I., 2010. Bloom dynamics and
537 life cycle strategies of two toxic dinoflagellates in a coastal upwelling system (NW Iberian
538 Peninsula). *Deep-Sea Res. Part II-Top. Stud. Oceanogr.* 57, 222–234.
539 <https://doi.org/10.1016/j.dsr2.2009.09.004>.

540

541 Briand, J.F., Djeridi, I., Jamet, D., Coupe, S., Bressy, C., Molmeret, M., Le Berre, B., Rimet, F.,
542 Bouchez, A., Blache, Y., 2012. Pioneer marine biofilms on artificial surfaces including
543 antifouling coatings immersed in two contrasting French Mediterranean coast sites.
544 *Biofouling* 28, 453. doi:10.1080/08927014.2012.688957.

545

546 Brissard, C., Herrenknecht, C., Séchet, V., Hervé, F., Pisapia, F., Harcouet, J., Lémée, R.,
547 Chomérat, N., Hess, P., Amzil, Z., 2014. Complex toxin profile of French Mediterranean
548 *Ostreopsis* cf. *ovata* strains, seafood accumulation and ovatoxins prepurification. *Mar. Drugs*
549 12, 2851–2876. doi:10.3390/md12052851.

550

551 Brown, M.A., Underwood, A. J., Chapman, M.G., Williams, R., Thompson, R.C., van Franeker,
552 J.A., 2015. Linking effects of anthropogenic debris to ecological impacts. *Proc. R. Soc. Ser. B.*
553 282, 20142929.

554

555 Ciminiello, P., Dell'Aversano, C., Dello Iacovo, E., Fattorusso, E., Forino, M., Grauso, L.,
556 Tartaglione, L., Guerrini, F., Pezzolesi, L., Pistocchi, R., Vanucci, S., 2012. Isolation and
557 structure elucidation of Ovatoxin-a, the major toxin produced by *Ostreopsis ovata*. *J. Am.*
558 *Chem. Soc.* 134, 1869–1875. <dx.doi.org/10.1021/ja210784u>.

559

560 Cole, M., Lindeque, P., Fileman, E., Halsband, C., Goodhead, R., Moger, J., Galloway, T.S., 2013.
561 Microplastic ingestion by zooplankton. *Environ. Sci. Technol.* 47, 6646-6655.
562 <dx.doi.org/10.1021/es400663f>.

- 563
564 Cózar, A., Echevarría, F., González-Gordillo, I.J., Irigoien, X., Úbeda, B., Hernández- Leónd, S.,
565 Palmae, A.T., Navarrof, S., García-de-Lomas, J., Ruizg, A., Fernández-de- Puelllesh, M.L.,
566 Duartei, C.M., 2014. Plastic debris in the open ocean. Proc. Natl. Acad. Sci. U. S. A. 111,
567 10239–10244. <https://doi.org/10.1073/pnas.1314705111>.
568
- 569 Derraik, J. G., 2002. The pollution of the marine environment by plastic debris: A review. Mar.
570 Pollut. Bull. 44, 842–852.
571
- 572 De Tender, C.A., Devriese, L.I., Haegeman, A., Maes, S., Ruttink, T., Dawyndt, P., 2015. Bacterial
573 Community Profiling of Plastic Litter in the Belgian Part of the North Sea. Environ. Sci.
574 Technol. 49, 9629–9638. doi: 10.1021/acs.est.5b01093.
575
- 576 Engler, R.E., 2012. The complex interaction between marine debris and toxic chemicals in the
577 ocean. Environ. Sci. Technol. 46, 12302–12315. [dx.doi.org/10.1021/es3027105](https://doi.org/10.1021/es3027105).
578
- 579 Eriksen, M., Lebreton, L.C.M., Carson, H.S., Thiel, M., Moore, C.J., et al., 2014. Plastic Pollution
580 in the World's Oceans: More than 5 Trillion Plastic Pieces Weighing over 250,000 Tons Afloat
581 at Sea. PLoS ONE 9(12), e111913. doi:10.1371/journal.pone.0111913.
582
- 583 Farrell, H., Brett, S., Ajani, P., Murray, S., 2013. Distribution of the genus *Alexandrium* (Halim)
584 and paralytic shellfish toxins along the coastline of New South Wales, Australia. Mar. Pollut.
585 Bull. 72, 133–145. <http://dx.doi.org/10.1016/j.marpolbul.2013.04.009>.
586
- 587 Fazey, F., M. C., Ryan, P. G., 2016. Biofouling on buoyant marine plastics : An experimental study
588 into the effect of size on surface longevity. Environ. Poll. 210, 354–360.
589 <https://doi.org/10.1016/j.envpol.2016.01.026>
- 590
- 591 Franco, J.M., Fernandez, P., Reguera, B., 1994. Toxin profiles of natural populations and cultures
592 of *Alexandrium minutum* Halim from Galician (Spain) coastal waters. J. Appl. Phycol. 6,
593 275–279.
594
- 595 Godhe, A., Asplund, M.E., Hårnström, K., Saravanan, V., Tyagi, A., Karunasagar, I., 2008.
596 Quantification of diatom and dinoflagellate biomasses in coastal marine seawater samples by
597 real-time PCR. Appl. Environm. Microbiol. 74, 7174–7182.
598 <https://doi.org/10.1128/AEM.01298-08>.
599
- 600 Goldstein, M.C., Carson, H.S., Eriksen, M., 2014. Relationship of diversity and habitat area in
601 North Pacific plastic-associated rafting communities. Mar. Biol. 161, 1441–1453. doi:
602 10.1007/s00227-014-2432-8.
603
- 604 Guillard, R.R.L., 1975. Culture of phytoplankton for feeding marine invertebrates, in: Smith, W.L.,
605 Chanley, M.H. (Eds.), Culture of Marine Invertebrates Animals. Plenum Press, New York, pp.
606 26–60.
607
- 608 Hallegraeff, G.M., 2010. Ocean climate change, phytoplankton community responses, and harmful
609 algal blooms: a formidable predictive challenge. J. Phycol. 46, 220-235.
610 <https://doi.org/10.1111/j.1529-8817.2010.00815.x>.
611

- 612 Hamer, J.P., Lucas, I.A.N., McCollin, T.A., 2001. Harmful dinoflagellate resting cysts in ships'
613 ballast tank sediments: potential for introduction into English and Welsh waters. *Phycologia*
614 40, 246–255. <https://doi.org/10.2216/i0031-8884-40-3-246.1>.
615
- 616 Ianora, A., Miralto, A., Poulet, S.A., Carotenuto, Y., Buttino, I., Romano, G., Casotti, R., Pohnert,
617 G., Wichard, T., Colucci-D'Amato, L., Terrazzano, G., Smetacek, V., 2004. Aldehyde
618 suppression of copepod recruitment in blooms of a ubiquitous planktonic diatom. *Nature* 429,
619 403–407.
620
- 621 Jambeck, J.R., Geyer, R., Wilcox, C., Siegler, T.R., Perryman, M., Andrady, A.L., Narayan, R.,
622 Law, K.L., 2015. Plastic waste inputs from land into the ocean. *Science* 346, 768e771.
623
- 624 Kiessling, T., Gutow, L., Thiel, M. 2015. Marine Litter as Habitat and Dispersal Vector. In:
625 Bergmann, M., Gutow, L., Klages, M. (Eds.), *Marine Anthropogenic Litter*. Springer
626 International Publishing, pp. 141-181.
627
- 628 Krock, B., Seguel, C.G., Cembella, A.D., 2007. Toxin profile of *Alexandrium catenella* from the
629 Chilean coast as determined by liquid chromatography with fluorescence detection and liquid
630 chromatography coupled with tandem mass spectrometry. *Harmful Algae* 6, 734–744.
631 doi:10.1016/j.hal.2007.02.005.
632
- 633 Kukulka, T., Proskurowski, G., Morét-Ferguson, S., Meyer, D.W., Law, K.L., 2012. The effect of
634 wind mixing on the vertical distribution of buoyant plastic debris. *Geophys. Res. Lett.* 39,
635 L07601. <https://doi.org/10.1029/2012GL051116>.
636
- 637 Lauritano, C., Romano, G., Roncalli, V., Amoresano, A., Fontanarosa, C., Bastianini, M., Braga, F.,
638 Carotenuto, Y., Ianora, A., 2016. New oxylipins produced at the end of a diatom bloom and
639 their effects on copepod reproductive success and gene expression levels. *Harmful Algae* 55,
640 221–229. <https://doi.org/10.1016/j.hal.2016.03.015>
641
- 642 Law, K.L., Morét-Ferguson, S., Maximenko, N.A., Proskurowski, G., Peacock, E.E., Hafner, J.,
643 Reddy, C.M., 2010. Plastic accumulation in the North Atlantic subtropical gyre. *Science* 329,
644 1185–1188. DOI: 10.1126/science.1192321.
645
- 646 Lebreton, L., Greer, S., Borrero, J., 2012. Numerical modeling of floating debris in the world's
647 oceans. *Mar. Poll. Bull.* 64, 653-661. <https://doi.org/10.1016/j.marpolbul.2011.10.027>.
648
- 649 Lobelle, D., Cunliffe, M., 2011. Early microbial biofilm formation on marine plastic debris. *Mar.*
650 *Pollut. Bull.* 62, 197-200. <https://doi.org/10.1016/j.marpolbul.2010.10.013>.
651
- 652 Masó, M., Fortuño, J.M., de Juan, S., Demestre, M., 2016. Microfouling communities from pelagic
653 and benthic marine plastic debris sampled across Mediterranean coastal waters. *Sci. Mar.* 80S1,
654 117-127. doi: <http://dx.doi.org/10.3989/scimar.04281.10A>.
655
- 656 Masó, M., Garcés, E., Pagés, F., Camp, J., 2003. Drifting plastic debris as a potential vector for
657 dispersing harmful algal bloom (HAB) species. *Sci. Mar.* 67, 107-111.
658 <https://doi.org/10.3989/scimar.2003.67n1107>.
659
- 660 Oberbeckmann, S., Loeder, M.G.J., Gerds, G., Osborn, A.M., 2014. Spatial and seasonal variation
661 in diversity and structure of microbial biofilms on marine plastics in Northern European waters.
662 *FEMS Microbiol. Ecol.* 90, 478-492. doi: 10.1111/1574-6941.12409.

- 663
664 Oberbeckmann, S., Martin, A.C., Löder, M.G.J., Labrenz, M., 2015. Marine microplastic-associated
665 biofilms – a review. *Environ. Chem.* 12, 551-562. <https://doi.org/10.1071/EN15069>.
666
- 667 Parsons, M. L., Aligizaki, K., Bottein, M. Y. D., Fraga, S., Morton, S. L., Penna, A., Rhodes, L.,
668 2012. *Gambierdiscus* and *Ostreopsis*: Reassessment of the state of knowledge of their
669 taxonomy, geography, ecophysiology, and toxicology. *Harmful Algae*, 14, 107–129.
670 <https://doi.org/10.1016/j.hal.2011.10.017>
671
- 672 Pegram, J.E., Andrady, A.L., 1989. Outdoor weathering of selected polymeric materials under
673 marine exposure conditions. *Polym. Degrad. Stabil.* 26, 333-345
674
- 675 Penna, A., Bertozzini, E., Battocchi, C., Galluzzi, L., Giacobbe, M.G., Vila, M., Garcés, E., Lugliè,
676 A., Magnani, M., 2007. Monitoring of HAB species in the Mediterranean Sea through
677 molecular methods. *J. Plankt. Res.* 29, 19-38. <https://doi.org/10.1093/plankt/fbl053>.
678
- 679 Penna, A., Casabianca, S., Perini, F., Bastianini, M., Riccardi, E., Pigozzi, S., Scardi, M., 2013.
680 Toxic *Pseudo-nitzschia* spp. in the northwestern Adriatic Sea: Characterization of species
681 composition by genetic and molecular quantitative analyses. *J. Plankt. Res.* 35, 352–366.
682 <https://doi.org/10.1093/plankt/fbs093>.
683
- 684 Penna, A., Garcés, E., Vila, M., Giacobbe, M.G., Fraga, S., Lugliè, A., Bravo, I., Bertozzini, E.,
685 Vernesi, C., 2005. *Alexandrium catenella* (Dinophyceae), a toxic ribotype expanding in the
686 NW Mediterranean Sea. *Mar. Biol.* 148, 13-23. <https://doi.org/10.1007/s00227-005-0067-5>.
687
- 688 Penna, A., Perini, F., Dell'Aversano, C., Capellacci, S., Tartaglione, L., Giacobbe, M.G.,
689 Casabianca, S., Fraga, S., Ciminiello, P., Scardi, M., 2015. The *sxt* gene and paralytic shellfish
690 poisoning toxins as markers for the monitoring of toxic *Alexandrium* species blooms. *Environ.*
691 *Sci. Technol.* 49, 14230-14238. <http://dx.doi.org/10.1021/acs.est.5b03298>.
692
- 693 Perini, F., Bastianini, M., Capellacci, S., Pugliese, L., DiPoi, E., Cabrini, M., Buratti, S., Marini,
694 M., Penna, A. 2018. Molecular methods for cost-efficient monitoring of HAB (harmful algal
695 bloom) dinoflagellate resting cysts. *Mar. Pollut. Bull.* (in press).
696
- 697 Perini, F., Galluzzi, L., Dell'Aversano, C., Dello Iacovo, E., Tartaglione, L., Ricci, F., Forino, M.,
698 Ciminiello, P., Penna, A., 2014. *SxtA* and *sxtG* Gene Expression and Toxin Production in the
699 Mediterranean *Alexandrium minutum* (Dinophyceae). *Mar. Drugs* 12, 5258–5276.
700 <https://doi.org/10.3390/md12105258>.
701
- 702 Perini, F., Casabianca, A., Battocchi, C., Accoroni, S., Totti, C., Penna, A., 2011. New approach
703 using the real-time PCR method for estimation of the toxic marine dinoflagellate *Ostreopsis* cf.
704 *ovata* in marine environment. *PLoS ONE* 6(3). <https://doi.org/10.1371/journal.pone.0017699>.
705
- 706 Pistocchi, R., Guerrini, F., Pezolesi, L., Riccardi, M., Vanucci, S., Ciminiello, P., Dell'Aversano,
707 C., Forino, M., Fattorusso, E., Tartaglione, L., Milandri, A., Pompei, M., Cangini, M., Pigozzi,
708 S., Riccardi, E., 2012. Toxin levels and profiles in microalgae from the north-Western Adriatic
709 Sea—15 years of studies on cultured species. *Mar. Drugs* 10, 140-162.
710 [doi:10.3390/md10010140](https://doi.org/10.3390/md10010140).
711
- 712 Reisser, J., Shaw, J., Hallegraef G., Proietti, M., Barnes, D.K., Thums, M., Wilcox, C., Hardesty,
713 B.D., Pattiaratchi, C., 2014. Millimeter- sized marine plastics: a new pelagic habitat for

- 714 microorganisms and invertebrates. PLoS One 9, e100289. doi:10.1371/JOURNAL.
715 PONE.0100289.
- 716
- 717 Rochman, C. M. 2015. The Complex Mixture, Fate and Toxicity of Chemicals Associated with
718 Plastic Debris in the Marine Environment. In: Bergmann, M., Gutow, L., Klages, M. (Eds.),
719 Marine
720 Anthropogenic Litter. Springer International Publishing, pp. 117-140.
- 721
- 722 Salta, M., Wharton, J. A., Blache, Y., Stokes, K. R., Briand, J. F. 2013. Marine biofilms on artificial
723 surfaces: structure and dynamics. Environ. Microbiol. 15, 2879.
- 724
- 725 Tartaglione, L., Dello Iacovo, E., Mazzeo, A., Casabianca, S., Ciminiello, P., Penna, A.,
726 Dell'Aversano, C., 2017. Variability in toxin profiles of the Mediterranean *Ostreopsis* cf. *ovata*
727 and in structural features of the produced ovatoxins. Environ. Sci. Technol. 51, 13920-13928.
728 doi: 10.1021/acs.est.7b03827.
- 729
- 730 Thiel, M., Gutow, L., 2005. The ecology of rafting in the marine environment. II. The rafting
731 organisms and community. Oceanogr. Mar. Biol. Annu. Rev. 43, 279-418.
- 732
- 733 Totti, C., Accoroni, S., Cerino, F., Cucchiari, E., Romagnoli, T., 2010. *Ostreopsis ovata* bloom
734 along the Conero Riviera (northern Adriatic Sea): relationships with environmental conditions
735 and substrata. Harmful Algae 9, 233–239.
- 736
- 737 Touzet, N., Franco, J.M., Raine, R., 2007. Characterization of non- toxic and toxin producing
738 populations of *Alexandrium minutum* (Dinophyceae) in Irish coastal waters. Appl. Environ.
739 Microb. 73, 3333–3342. doi:10.1128/AEM.02161-06.
- 740
- 741 Trainer, V.L., Bates, S.S., Lundholm, N., Thessen, A.E., Cochlan, W.P., Adams, N.G., Trick, C.G.,
742 2012. *Pseudo-nitzschia* physiological ecology, phylogeny, toxicity, monitoring and impacts on
743 ecosystem health. Harmful Algae 14, 271–300. <https://doi.org/10.1016/j.hal.2011.10.025>.
- 744
- 745 Turner, A.D., Dhanji-Rapkova, M., Rowland-Pilgrim, S., Turner, L.M., Rai, A., Venugopal, M.N.,
746 Karunasagar, I., Godhe, A., 2017. Assessing the presence of marine toxins in bivalve molluscs
747 from southwest India. Toxicon 140, 147-156. doi: 10.1016/j.toxicon.2017.11.001.
- 748
- 749 Vila, M., Giacobbe, M.G., Masó, M., Gangemi, E., Penna, A., Sampedro, N., Azzaro, M., Camp, J.,
750 Galluzzi, L., 2005. A comparative study on recurrent blooms of *Alexandrium minutum* in two
751 Mediterranean coastal areas. Harmful Algae 4, 673-695.
752 <https://doi.org/10.1016/j.hal.2004.07.006>.
- 753
- 754 Webb, H.K., Crawford, R.J., Sawabe, T., Ivanova, E.P., 2009. Poly(ethylene terephthalate) polymer
755 surfaces as a substrate for bacterial attachment and biofilm formation. Microbes Environ. 24,
756 39. doi:10.1264/JSME2.ME08538.
- 757
- 758 Wood, A.M., Everroad, R.C., Wingard, L.M., 2005. Measuring growth rates in microalgal cultures,
759 in: Anderson, R.A. (Ed.), Algal Culturing Techniques. Elsevier Academic Press, London, pp.
760 269–286.
- 761
- 762 Zettler, E.R., Mincer, T.J., Amaral-Zettler, L.A., 2013. Life in the ‘plastisphere’: Microbial
763 communities on plastic marine debris. Environ. Sci. Technol. 47, 7137–7146.
764 [dx.doi.org/10.1021/es401288x](https://doi.org/10.1021/es401288x).

765
766

767 Table 1. Individual and total toxin content on a per cell basis (fg cell⁻¹) of the Mediterranean *Alexandrium pacificum*
 768 strains.

769 Strains	C1	C2	dcGTX2	dcGTX3	GTX2	GTX3	GTX1	GTX4	GTX5	STX	NEO	dc-NEO	Total
771 CNR-ACAT 5D1	ND	ND	ND	ND	1.63	ND	19.93	ND	13.28	0.29	ND	ND	35.14
772 CNR-ACAT6A2	ND	18.97	ND	ND	ND	ND	13.01	4.78	1.70	5.12	ND	ND	43.58
773 CNR-ACAT6FA	26.62	1413.22	ND	ND	10.11	ND	422.68	181.11	3978.50	ND	ND	ND	6032.25
774 CNR-ACAT15	3.84	117.76	ND	ND	13.11	70.11	217.57	66.80	320.68	ND	ND	ND	809.87
775 CNR-ACAT6D4	4.38	432.41	ND	ND	15.23	342.02	247.95	79.97	444.13	18.04	ND	ND	1584.12
776 CNR-ACATA1	1.77	160.00	ND	ND	10.08	2.45	227.03	64.99	139.56	3.21	ND	ND	609.09
777 CNR-ACAT7A2	0.74	114.74	ND	ND	1.13	ND	45.39	23.23	71.81	ND	ND	ND	257.04
778 CNR-ACAT02	52.97	388.20	ND	ND	1.13	3.62	119.66	112.31	ND	1.11	10.263	ND	689.26
779 CNR-ACAT6D5	32.31	887.33	1.15	ND	35.55	ND	ND	ND	844.77	ND	ND	ND	1801.11
780 CNR-ACAT15P	6.52	148.76	ND	ND	4.62	ND	103.19	57.90	250.08	ND	ND	ND	571.08

781 ND, not detectable.

782

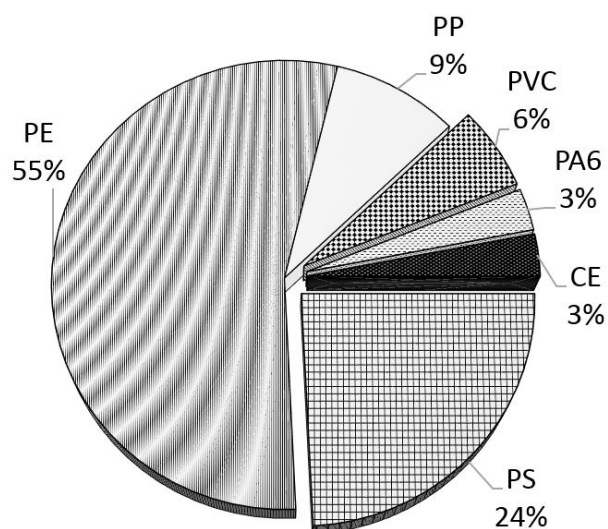
783

784

785

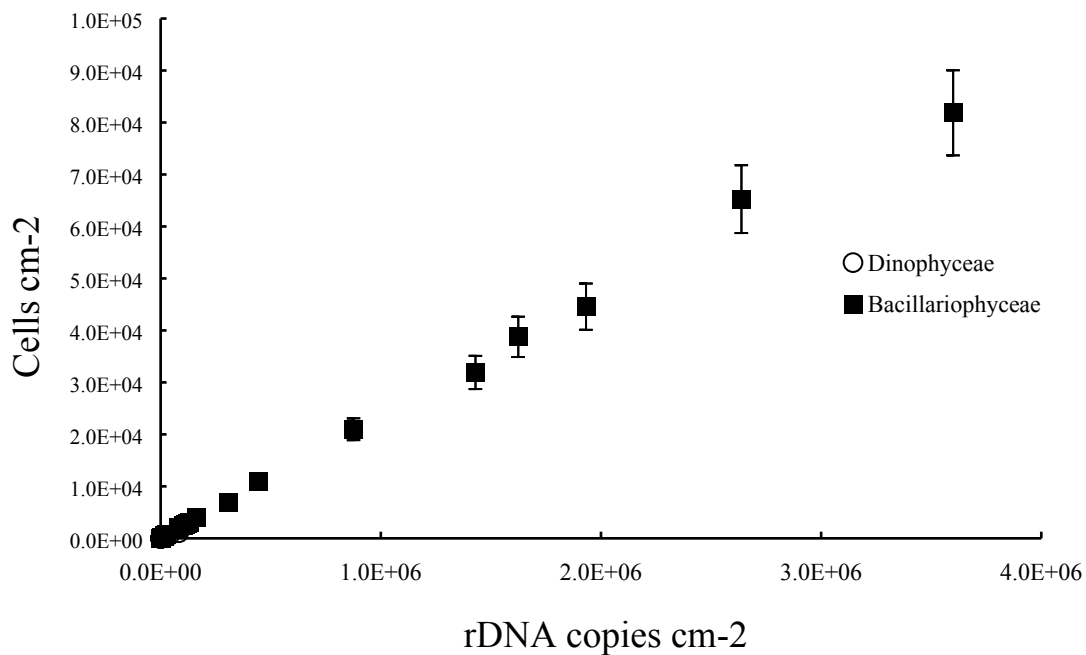
786

787



788
789
790
791
792
793
794
795
796
797
798
799
800

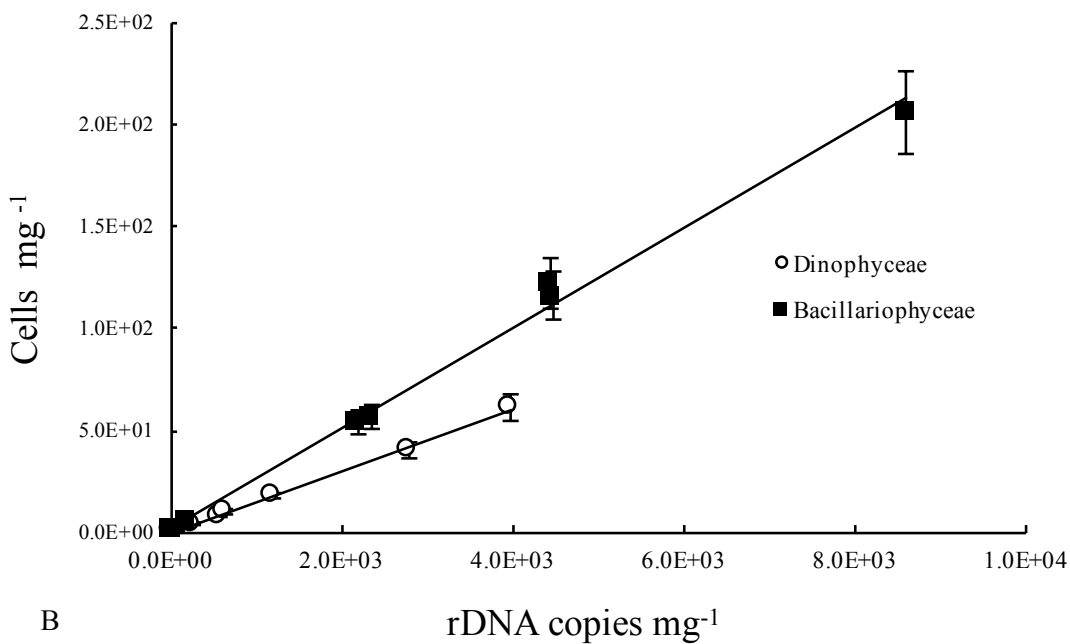
Figure 1. Polymer identification by ATR-FTIR. Identification analysis of plastic samples were expressed as percentage amount. PE: polyethylene; PP: polypropylene; PVC: polyvinylchloride; PA 6: polyamide 6; CE: cellulose; PS: polystyrene. Sectors with grid indicated polar and amorphous polymers. Chemical structures of the polymers were reported in Table S5 of the supplementary material.



801

V

802

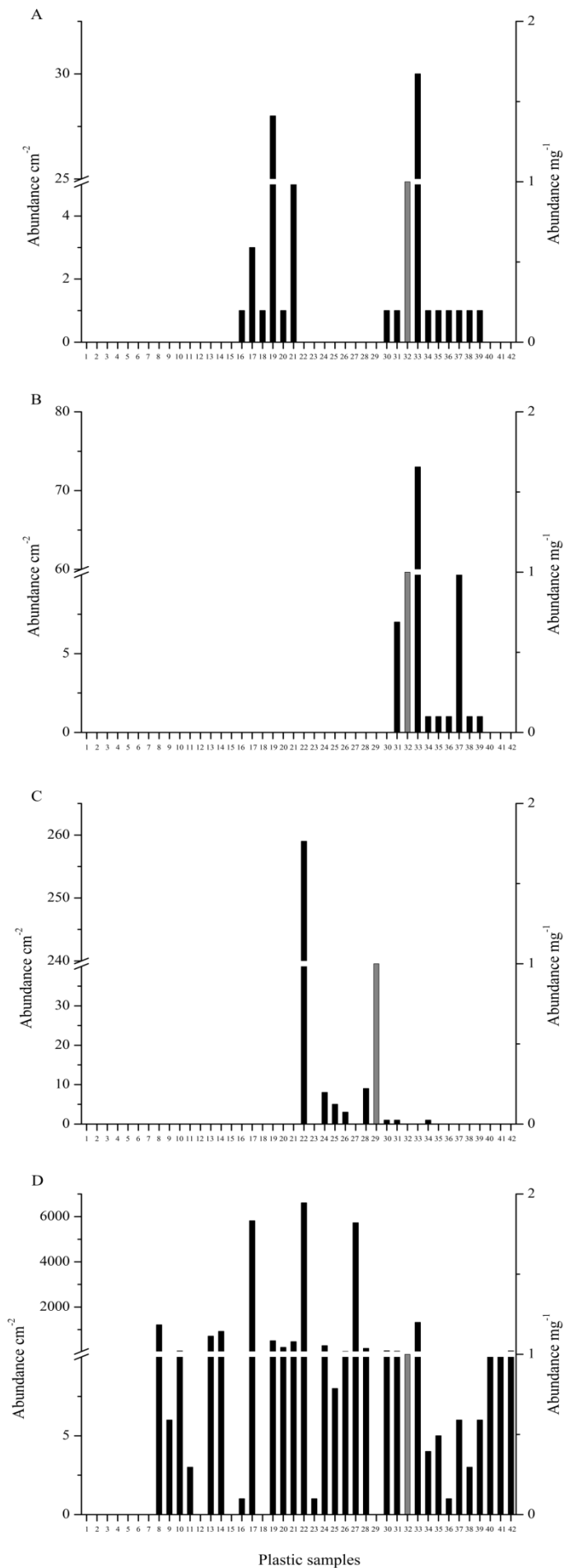


B

803

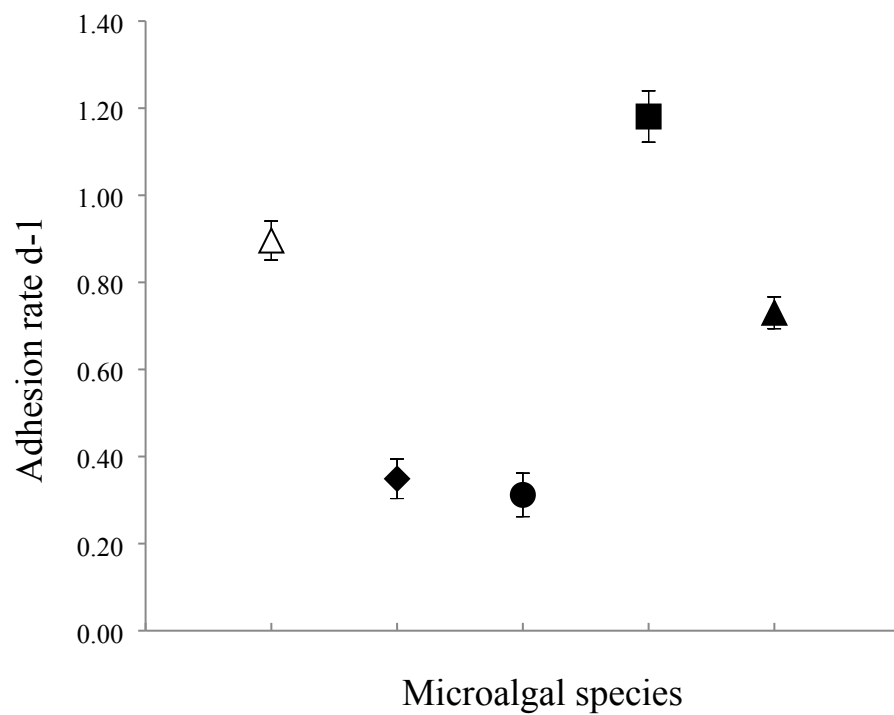
804

805 Figure 2. Linear relationship between Bacillariophyceae and Dinophyceae abundance expressed as
 806 (A) cells cm⁻² and rDNA gene content (copies cm⁻²) or (B) cells mg⁻¹ and rDNA gene content
 807 (copies mg⁻¹) determined on various plastic substrates using the qPCR assay. Two different cellular
 808 standard curves were used for diatom and dinoflagellate cellular estimation. Bacillariophyceae and
 809 Dinophyceae rDNA gene copy number were determined using standard curves from purified SSU
 810 rDNA PCR products. Linear correlations between Bacillariophyceae and Dinophyceae abundance
 811 and rDNA gene content were high and significant ($p < 0.01$).



813 Figure 3. Molecular quantification of target harmful microalgal species abundance on plastic
814 samples collected in the Mediterranean Sea in 2016-2017 period by qPCR assay. (A) *Alexandrium*
815 *pacificum*, (B) *A. minutum*, (C) *Ostreopsis* cf. *ovata*, (D) *Pseudo-nitzschia* spp. Black columns
816 indicate abundance cm^{-2} ; grey columns indicate abundance mg^{-1} . One cell mg^{-1} was detected in
817 samples n. 29 for *O.* cf. *ovata* and n. 32 for *A. pacificum*, *A. minutum* and *Pseudo-nitzschia* spp.
818 Note the y axis break in all graphs.
819
820

821
822
823
824
825
826
827
828



829
830
831
832
833
834
835
836
837
838

Figure 4. Adhesion rates of different cultured harmful microalgal strains to the plastic surfaces (means \pm SD, n = 3). *Alexandrium pacificum* (■), *Skeletonema marinoi* (△), *Pseudo-nitzschia multistriata* (▲), *Alexandrium minutum* (◆) and *Ostreopsis cf. ovata* (●).

Supporting Information

Plastics as Vectors for Potentially Harmful Algal Species Dispersal in marine Environment

by Silvia Casabianca, Samuela Capellacci, Maria Grazia Giacobbe, Carmela Dell'Aversano, Fabio Varrale, Luciana Tartaglione, Riccardo Narizzano, Fulvia Risso, Paolo Moretto, Alessandro Dagnino, Rosella Bertolotto, Enrico Barbone, Nicola Ungaro, Antonella Penna

Table S1: Microalgal strains used for plastics adhesion experiments, molecular standard curves in the qPCR assay or chemical analysis of LC-HRMS.

Table S2: Environmental plastic samples collected in the Mediterranean Sea.

Table S3: Primers used for the amplification of SSU, ITS-5.8S and LSU rDNA of microalgal taxa, and SSU rDNA of bacteria

Table S4: Percentage of various Dinophyceae and Bacillariophyceae DNAs mixtures set up (see also Materials and Methods). Each mixture was a combination of various amounts of DNA for building up the mixed standard curves to quantify the abundance of Dinophyceae and Bacillariophyceae.

Table S5: Chemical structure of the identified polymers in plastic samples.

Fig. S1. ATR-FTIR spectrum of Polyethylene of analyzed plastic samples.

Fig. S2. ATR-FTIR spectrum of Polypropylene of analyzed plastic samples.

Fig. S3. ATR-FTIR spectrum of Polystyrene of analyzed plastic samples.

Fig. S4. ATR-FTIR spectrum of Polyvinylchloride of analyzed plastic samples.

Fig. S5. ATR-FTIR spectrum of Polyamide 6 of analyzed plastic samples.

Fig. S6. ATR-FTIR spectrum of Cellulose of analyzed plastic samples.

Table S1. Microalgal strains used for plastic adhesion experiments, molecular standard curves in the qPCR assay or chemical analysis of LC-HRMS.

Species	Strain	Class	Medium	Analysis
<i>Alexandrium andersoni</i>	VGO664	Dinophyceae	f/2	molecular
<i>Alexandrium minutum</i>	CBA57	Dinophyceae	f/2	adhesion/molecular
<i>Alexandrium pacificum</i>	CNR-SRA4	Dinophyceae	f/2	adhesion/molecular
<i>Alexandrium pacificum</i>	CNR-ACAT5D1	Dinophyceae	f/2	chemical
<i>Alexandrium pacificum</i>	CNR-ACAT6A2	Dinophyceae	f/2	chemical
<i>Alexandrium pacificum</i>	CNR-ACAT6FA	Dinophyceae	f/2	chemical
<i>Alexandrium pacificum</i>	CNR-ACAT15	Dinophyceae	f/2	chemical
<i>Alexandrium pacificum</i>	CNR-ACAT6D4	Dinophyceae	f/2	chemical
<i>Alexandrium pacificum</i>	CNR-ACATA1	Dinophyceae	f/2	chemical
<i>Alexandrium pacificum</i>	CNR-ACAT7A2	Dinophyceae	f/2	chemical
<i>Alexandrium pacificum</i>	CNR-ACAT02	Dinophyceae	f/2	chemical
<i>Alexandrium pacificum</i>	CNR-ACAT6D5	Dinophyceae	f/2	chemical
<i>Alexandrium pacificum</i>	CNR-ACAT15P	Dinophyceae	f/2	chemical
<i>Coolia monotis</i>	CBA1	Dinophyceae	f/4	molecular
<i>Gonyaulax spinifera</i>	CBA5	Dinophyceae	f/4	adhesion/molecular
<i>Heterocapsa</i> sp.	CBAB/D5	Dinophyceae	f/2	molecular
<i>Lingulodinium polyedrum</i>	LPA0510	Dinophyceae	f/10	adhesion/molecular
<i>Ostreopsis</i> cf. <i>ovata</i>	CBA1291	Dinophyceae	f/4	adhesion/molecular
<i>Prorocentrum lima</i>	CBA3	Dinophyceae	f/4	molecular
<i>Protoceratium reticulatum</i>	PRA0311	Dinophyceae	f/4	adhesion
<i>Scrippsiella</i> sp.	CBA1	Dinophyceae	f/2	molecular
<i>Chaetoceros</i> sp.	CBA22	Bacillariophyceae	f/2 with Si	molecular
<i>Cylindroteca</i> sp.	CBA7	Bacillariophyceae	f/2 with Si	molecular
<i>Coscinodiscus</i> sp.	CBA1	Bacillariophyceae	f/2 with Si	molecular
<i>Guinardia flaccida</i>	CBA1	Bacillariophyceae	f/2 with Si	molecular
<i>Pseudo-nitzschia</i> cf. <i>arenysensis</i>	CBA163	Bacillariophyceae	f/2 with Si	molecular
<i>Pseudo-nitzschia calliantha</i>	CBA189	Bacillariophyceae	f/2 with Si	molecular
<i>Pseudo-nitzschia multistriata</i>	CBA174	Bacillariophyceae	f/2 with Si	adhesion
<i>Pseudo-nitzschia pungens</i>	CBA180	Bacillariophyceae	f/2 with Si	molecular
<i>Skeletonema marinoi</i>	CBA4	Bacillariophyceae	f/2 with Si	adhesion/molecular
<i>Thalassionema</i> sp.	CBA10	Bacillariophyceae	f/2 with Si	molecular
<i>Thalassiosira</i> sp.	CBA1	Bacillariophyceae	f/2 with Si	molecular

Table S2. List and properties of environmental plastic samples collected in the Mediterranean Sea.

Sample ID	Sampling date	Regional Sea	Location	Geographic Coordinates	Polymer type	Sample size
1	15 th March 2016		Genova - Voltri	44°25'4.15"N; 8°45'59.03"E	PE	220 mg
2	15 th March 2016		Genova - Voltri	44°25'4.15"N; 8°45'59.03"E	PE	260 mg
3	26 th September 2016	Ligurian Sea	Genova - Voltri	44°24'54.17"N; 8°46'0.03"E	PE	400 mg
4	26 th September 2016		Genova - Voltri	44°24'54.17"N; 8°46'0.03"E	PE	350 mg
5	26 th September 2016		Genova - Voltri	44°24'54.17"N; 8°46'0.03"E	PE	95 mg
6	17 th May 2016		Fano	43°49'59.55"N; 13°03'38.23"E	PE	2.3 cm ²
7	17 th May 2016		Fano	43°49'59.55"N; 13°03'38.23"E	PE	6.3 cm ²
8	22 th May 2016		Pesaro	43°56'32.31"N; 13°58'18.04"E	PS	5 cm ²
9	1 st July 2016		Pesaro harbour	43°55'41.78"N; 12°53'09.77"E	PE	24 cm ²
10	1 st July 2016		Pesaro harbour	43°55'41.78"N; 12°53'09.77"E	PE	40 cm ²
11	1 st July 2016		Croce Pesaro	43°55'41.78"N; 12°53'09.77"E	PP	70 cm ²
12	1 st July 2016		Croce Pesaro	43°55'41.78"N; 12°53'09.77"E	PE	12 cm ²
13	4 th August 2016	Adriatic Sea	Fano	43°52'05.21"N; 13°00'56.61"E	PS	4 cm ²
14	4 th August 2016		Fosso Sejore	43°53'05.79"N; 12°58'18.04"E	PS	4.5 cm ²
15	19 th October 2016		Bari	41°7'44.36"N; 16°57'10.73"E	PE	188 mg
16	19 th October 2016		Bari	41°7'44.36"N; 16°57'10.73"E	PE	60 cm ²

17	15 th May 2016	Siracusa	37°03'50.21"N; 15°17'4.53"E	PS	4.5 cm ²
18	15 th May 2016	Siracusa	37°03'50.21"N; 15°17'4.53"E	PS	4 cm ²
19	26 th May 2016	Siracusa	37°03'52.32"N; 15°16'47.52"E	PE	5 cm ²
20	26 th May 2016	Siracusa	37°03'51.71"N; 15°16'48.71"E	n.a.	8 cm ²
21	26 th May 2016	Siracusa	37°03'51.71"N; 15°16'48.71"E	PS	6 cm ²
22	4 th September 2016	Isolabella	37°51'0.99"N; 15°18'2.93"E	CE	1.7 cm ²
23	4 th September 2016	Lido Mendolia	37°51'8.94"N; 15°18'0.52"E	PE	15 cm ²
24	4 th September 2016	Isolabella Diving	37°51'10.40"N; 15°18'6.28"E	PVC	24 cm ²
25	4 th September 2016	Isolabella Diving	37°51'10.20"N; 15°18'7.17"E	PE	16 cm ²
26	4 th September 2016	Isolabella Diving	37°51'09.55"N; 15°18'7.13"E	PE	12 cm ²
27	4 th September 2016	Isolabella	37°51'0.99"N; 15°18'2.93"E	PA	7.5 cm ²
28	4 th September 2016	Isolabella	37°51'0.99"N; 15°18'2.93"E	PA	12 cm ²
29	26 th October 2016	Porto Cesareo	40°13'41.99"N; 17°51'54.07"E	PE	210 mg
30	26 th October 2016	Porto Cesareo	40°13'41.99"N; 17°51'54.07"E	PE	42 cm ²
31	19 th April 2017	SR small Port	37°04'2.29"N; 15°17'19.63"E	PS	4.3 cm ²
32	19 th April 2017	SR big Port	37°03'48.94"N; 15°16'52.46"E	PE	250 mg
33	19 th April 2017	SR small Port	37°04'2.29"N; 15°17'19.63"E	PS	3.9 cm ²
34	19 th April 2017	SR small Port	37°04'2.29"N; 15°17'19.63"E	PVC	36 cm ²
35	7 th May 2017	Circolo Nautico	37°04'2.29"N; 15°17'19.63"E	PS	22 cm ²

Ionian Sea

36	7 th May 2017	Cantiere nautico	37°03'54.18"N; 15°16'48.94"E	PE	80 cm ²
37	7 th May 2017	Cantiere nautico	37°03'51.71"N; 15°16'48.71"E	PS	13 cm ²
38	7 th May 2017	SR small Port	37°04'8.14"N; 15°17'28.24"E	PE	18 cm ²
39	7 th May 2017	SR small Port	37°04'8.14"N; 15°17'28.24"E	PS	14.5 cm ²
Tyrrhenian Sea					
40	18 th August 2016	Lipari	38°27'18.47"N; 14°55'58.80"E	PE	60 cm ²
41	18 th August 2016	Lipari	38°27'34.85"N; 14°55'57.25"E	PE	54 cm ²
42	18 th August 2016	Lipari	38°27'39.81"N; 14°55'20.71"E	PE	2.5 cm ²

PE, Polyethylene; PS, Polystyrene; CE, Cellulose; PVC, Polyvinylchloride; PA, Polyamides
na, not analyzed

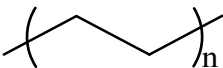
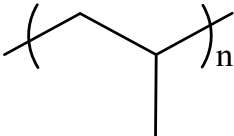
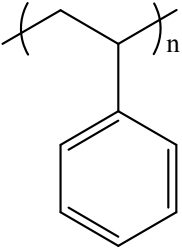
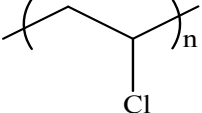
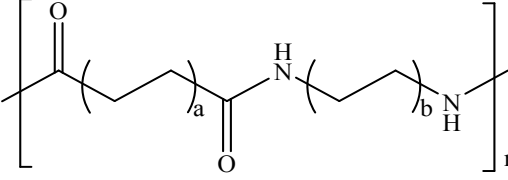
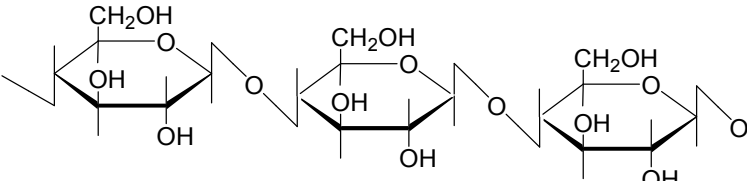
Table S3. Primers used for the amplification of SSU, 5.8S-ITS and LSU rDNA of microalgal taxa.

Target	Primer	Sequence	Primer location	Primer concentration [nM]	Reference
Dinophyceae	EUK528f	Forward 5'-CCGCGGTAATTCCAGCTC-3'	SSU	300	Godhe et al., 2008
	Dino18SR1	Reverse 5'-GAGCCAGATRCDCACCCA-3'	SSU	300	
Bacillariophyceae	1209f	Forward 5'-CAGGTCTGTGATGCCCTT-3'	SSU	300	Godhe et al., 2008
	Diatom18SR1	Reverse 5'-CAATGCAGWTTGATGAWCTG-3'	SSU	300	
<i>Alexandrium minutum</i>	ITS1m	Forward 5'-CATGCTGCTGTGTTGATGACC-3'	ITS1	200	Penna et al., 2007
	5.8S-3'	Reverse 5'-GCAMACCTTCAAGMATATCCC-3'	5.8S	200	
<i>Alexandrium pacificum</i>	ITS1p	Forward 5'-AGCATGATTTGTTTTCAAGC-3'	ITS1	200	Penna et al., 2007
	5.8S-3'	Reverse 5'-GCAMACCTTCAAGMATATCCC-3'	5.8S	200	
<i>Gonyaulax spinifera</i>	GspinF_for	Forward 5'-GAAACTCCTTCTGTGGATGC-3'	LSU	200	Perini et al., 2018
	GspinR_rev	Reverse 5'-TCACAGTTCCTCATGGTACT-3'	LSU	200	
<i>Lingulodinium polyedrum</i>	Lpoly RT-for	Forward 5'-AACTCGTTGGCGAGCATTTT-3'	ITS2	400	Perini et al., 2018
	Lpoly RT-rev	Reverse 5'-CGCTAGCAAAGCACTCGCTTA-3'	ITS2	400	
<i>Ostreopsis cf. ovata</i>	Ovata rt F	Forward 5'-TTTGATCACTTTGGCAATCT-3'	LSU	300	Perini et al., 2011
	Ovata rt R	Reverse 5'-TGAACCTTACCATGCCATTAG-3'	LSU	300	
<i>Protoceratium reticulatum</i>	Pret RT-for	Forward 5'-GGTGCAGTGAAATGTATTAGGCATT-3'	5.8S	200	Perini et al., 2018
	Pret RT-rev	Reverse 5'-TCCCAAAAACATAGAATACGTTCAAT-3'	5.8S	200	
<i>Pseudo-nitzschia</i> spp.	Pseudo 5'	Forward 5'-CGATACGTAATGCGAATTGCAA-3'	5.8S	300	Penna et al., 2007
	Pseudo 3'	Reverse 5'-GTGGGATCCRCAGACACTCAGA-3'	5.8S	300	

Table S4. Percentage of various Dinophyceae and Bacillariophyceae DNAs mixtures set up (see also Materials and Methods). Each mixture was a combination of various amounts of DNA for building up the mixed standard curves to quantify the abundance of Dinophyceae and Bacillariophyceae.

	Percentage DNA of <i>Alexandrium andersonii</i>	Percentage DNA of <i>Coolia monotis</i>	Percentage DNA of <i>Scrippsiella</i> sp.	Percentage DNA of <i>Ostreopsis cf. ovata</i>	Percentage DNA of <i>Gonyaulax spinifera</i>
Mixture					
A	20	20	20	20	20
B	20	10	10	20	40
C	10	20	20	40	10
D	20	10	40	10	20
E	40	20	10	20	10
F	10	40	20	10	20
	<i>Heterocapsa</i> sp.	<i>Lingulodinium polyedrum</i>	<i>Prorocentrum lima</i>	<i>Alexandrium minutum</i>	<i>Alexandrium pacificum</i>
Mixture					
G	20	20	20	20	20
H	20	10	10	20	40
I	10	20	20	40	10
L	20	10	40	10	20
M	40	20	10	20	10
N	10	40	20	10	20
	<i>Pseudo-nitzschia pungens</i>	<i>Chaetoceros</i> sp.	<i>Thalassionema</i> sp.	<i>Skeletonema marinoi</i>	<i>Cylindroteca</i> sp.
Mixture					
A'	20	20	20	20	20
B'	40	20	10	20	10
C'	20	10	10	20	40
D'	20	10	40	10	20
E'	40	20	10	20	10
F'	10	40	20	10	20
	<i>Guinardia flaccida</i>	<i>Pseudo-nitzschia calliantha</i>	<i>Coscinodiscus</i> sp.	<i>Pseudo-nitzschia cf. arenysensis</i>	<i>Thalassiosira</i> sp.
Mixture					
G'	20	20	20	20	20
H'	20	10	10	20	40
I'	10	20	20	40	10
L'	20	10	40	10	20
M'	40	20	10	20	10
N'	10	40	20	10	20

Table S5. Chemical structure of the identified polymers in plastic samples.

Polymer	Chemical structure
Polyethylene (PE)	
Polypropylene (PE)	
Polystyrene (PS)	
Polyvinylchloride (PVC)	
Polyamides (PA) All polyamides; a, b vary from 0 to 12 based on monomer type.	
Cellulose (CE)	

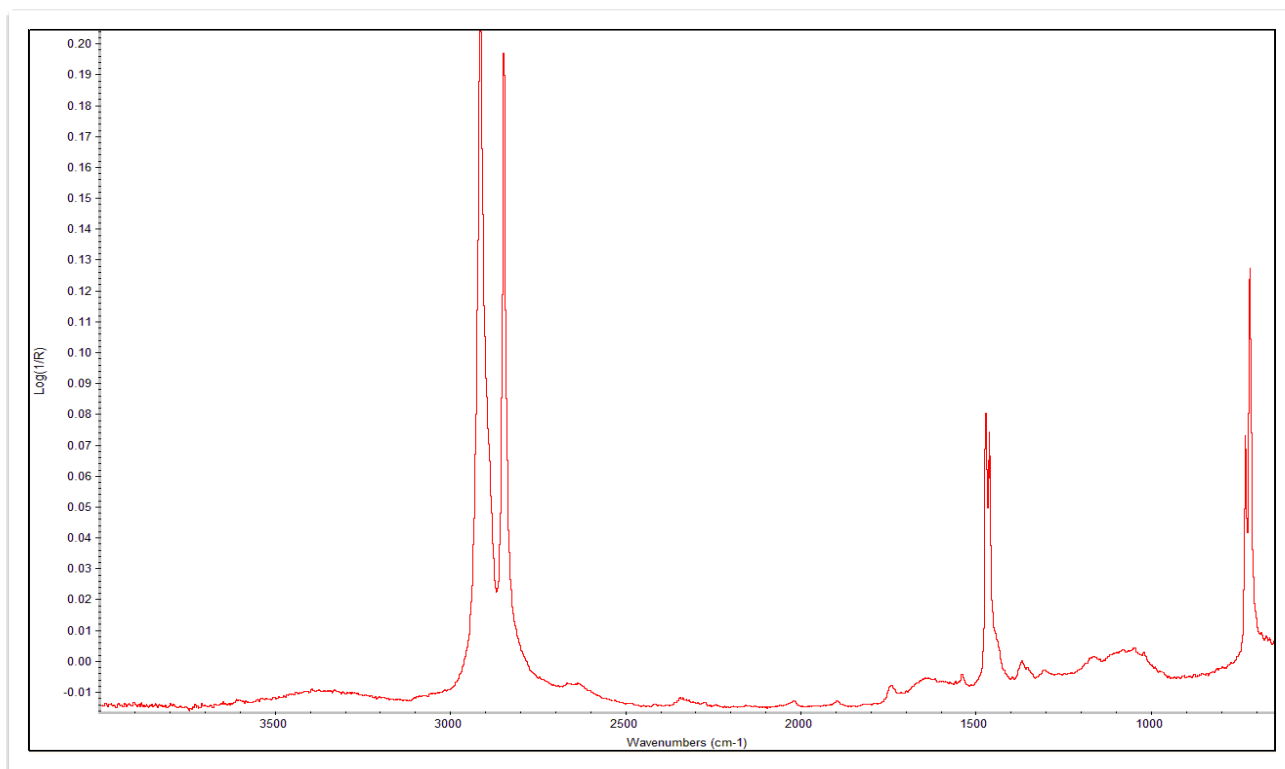


Fig. S1. ATR-FTIR spectrum of Polyethylene of analyzed plastic samples.

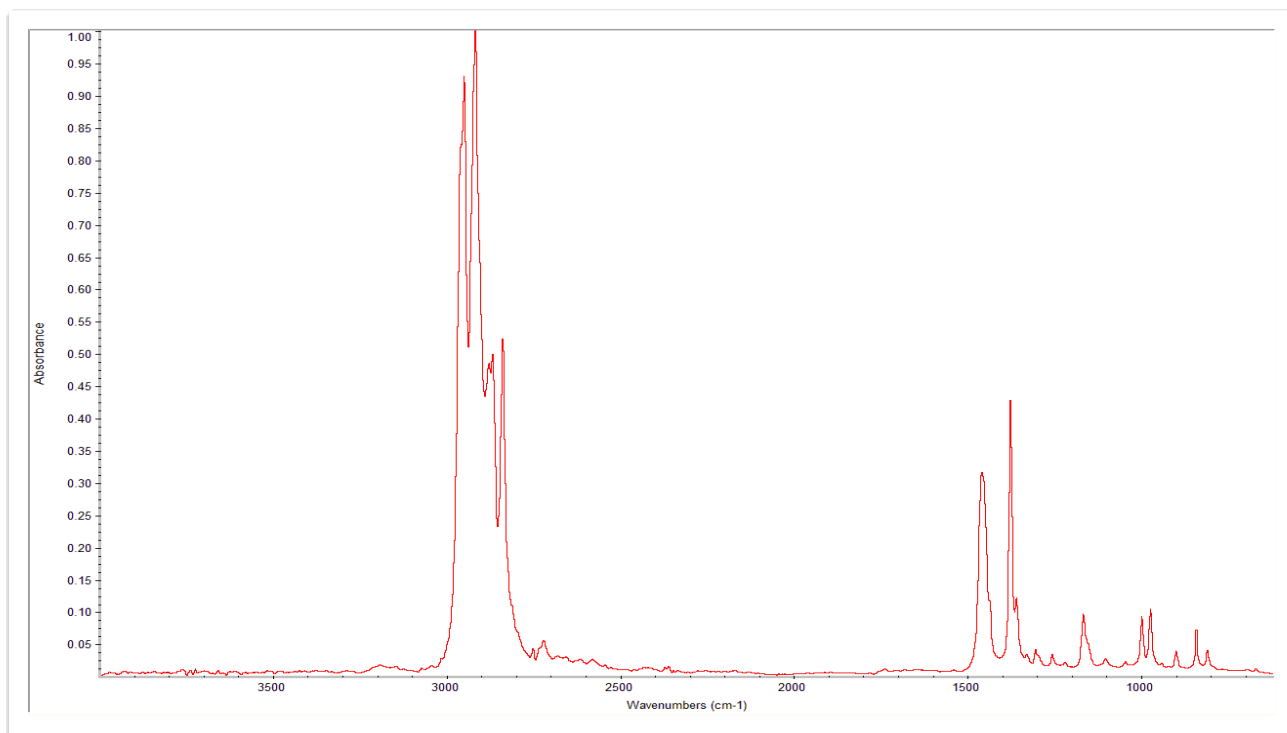


Fig. S2. ATR-FTIR spectrum of Polypropylene of analyzed plastic samples.

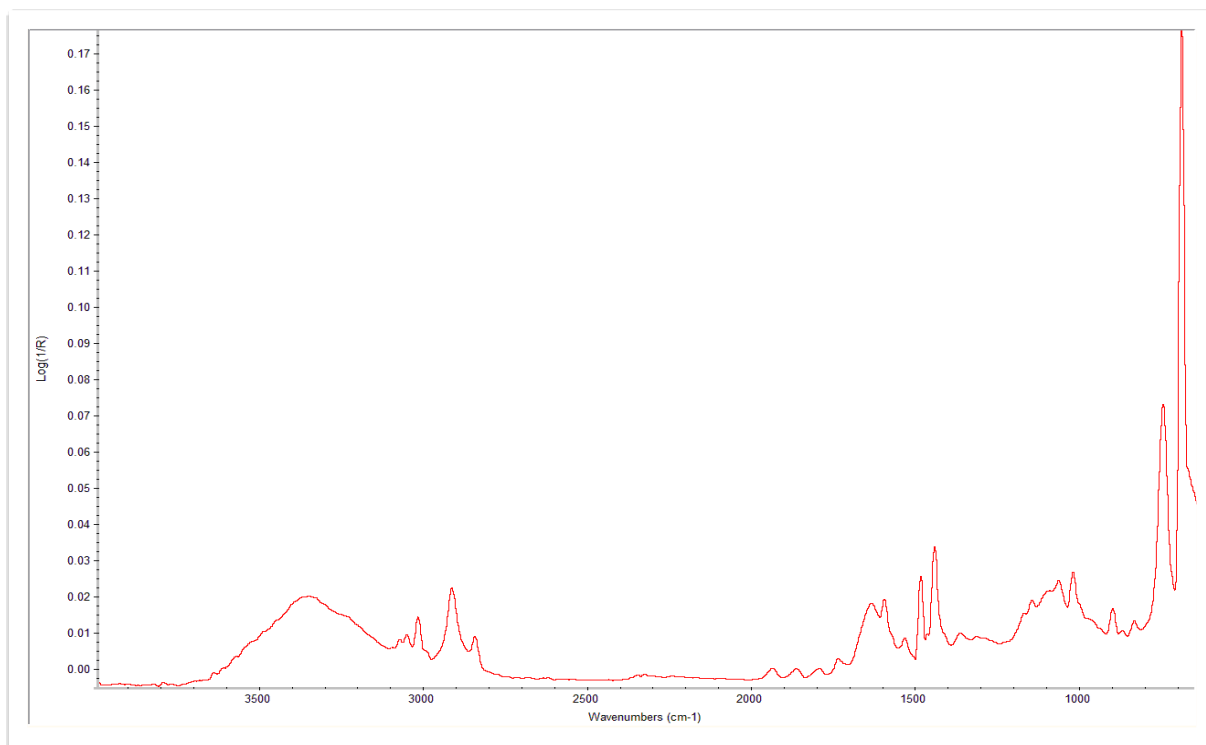


Fig. S3. ATR-FTIR spectrum of Polystyrene of analyzed plastic samples.

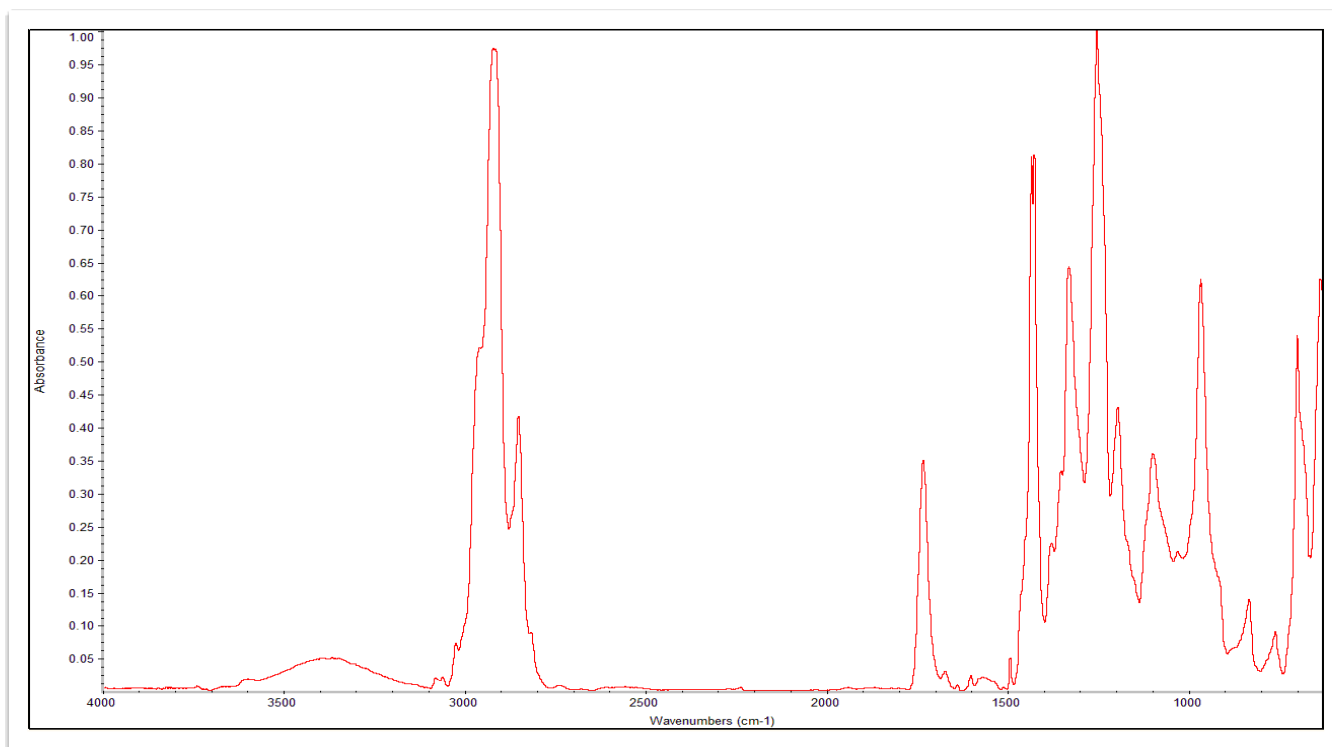


Fig. S4. ATR-FTIR spectrum of Polyvinylchloride of analyzed plastic samples.

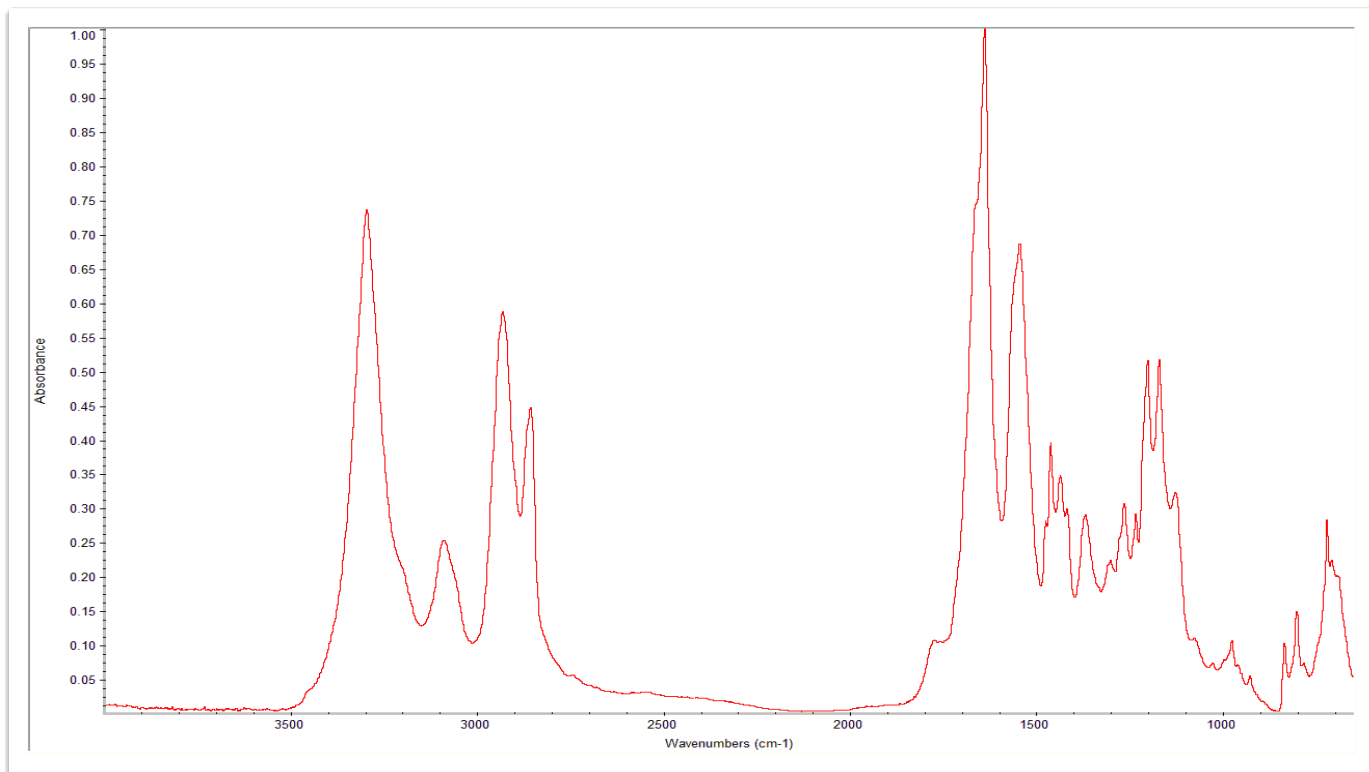


Fig. S5. ATR-FTIR spectrum of Polyamide 6 of analyzed plastic samples.

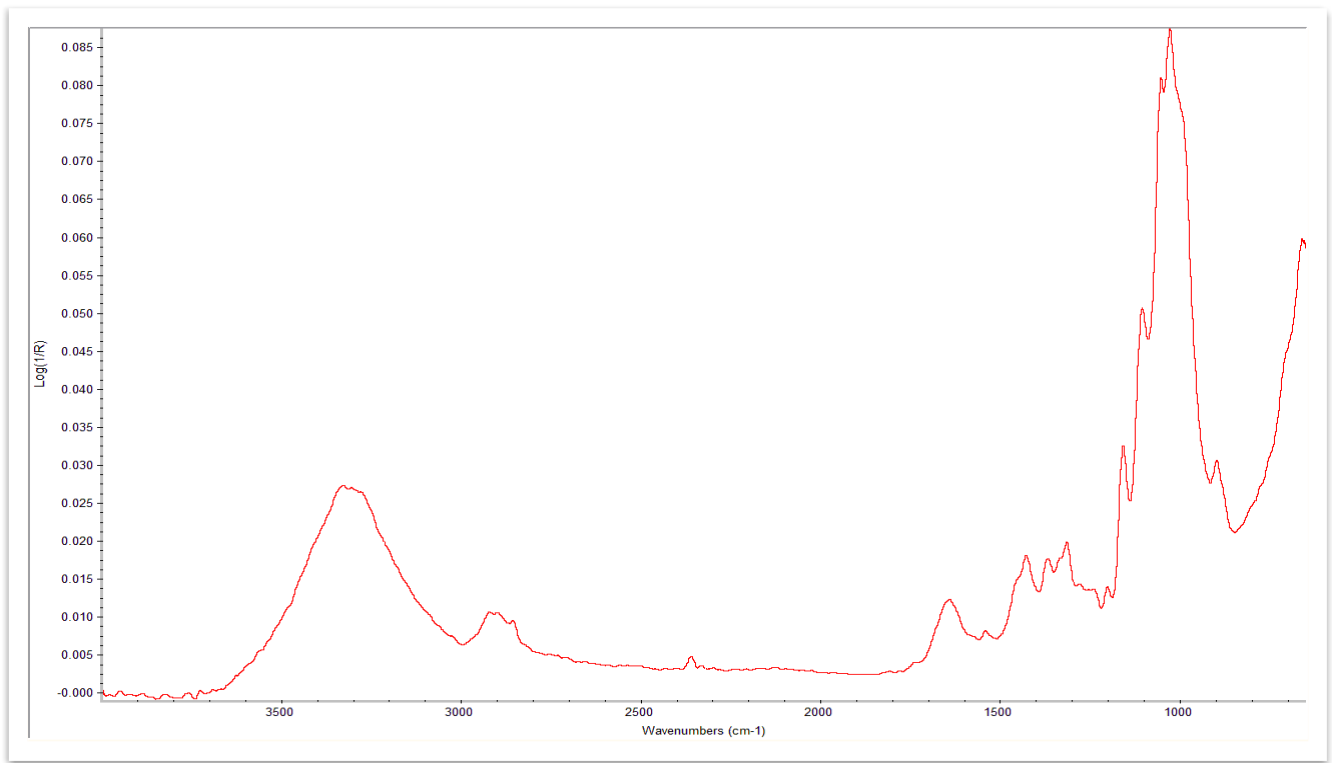


Fig. S6. ATR-FTIR spectrum of Cellulose of analyzed plastic samples.